MODELS AND OBSERVATIONS OF THE CHEMISTRY NEAR YOUNG STELLAR OBJECTS

EWINE F. VAN DISHOECK
Leiden Observatory P.O. Box 9513
2300 RA Leiden, The Netherlands
e-mail: ewine@strw.leidenuniv.nl

AND

MICHIEL R. HOGERHEIJDE
Astronomy Department, Univ. of California
Berkeley, CA 94720, USA
e-mail: michiel@astro.berkeley.edu

1. Introduction

The study of the chemical evolution of gas and dust from pre-stellar dense cores to circumstellar disks around young stars forms an essential part of understanding star- and planet formation. Throughout the collapse- and protostellar phases, simple and complex molecules are formed, many of which deplete onto cold grains and are eventually incorporated into the icy planetesimals of new solar systems (see Figure 1). Tracing this chemical evolution provides a wealth of information, not only about the chemical processing in primitive solar nebulae, but also about physical processes which occur in the immediate surroundings of young stellar objects (YSOs).

Interstellar chemistry has been an active field of research for more than 60 years, ever since the detection of the first molecules in 1937–1941. Nearly 120 different gas-phase species have been identified (see Table 1), not including isotopic varieties, with abundances down to 10^{-11} with respect to H_2. The majority of the species have been detected through their rotational transitions at millimeter wavelengths. Most of the early observations were performed with typical beam sizes of $1'$, corresponding to linear scales of nearly 10,000 AU (0.04 pc) in the nearest star-forming regions in Taurus and Ophiuchus. With the advent of large single-dish submillimeter telescopes and millimeter interferometers, it has become possible to study the dense

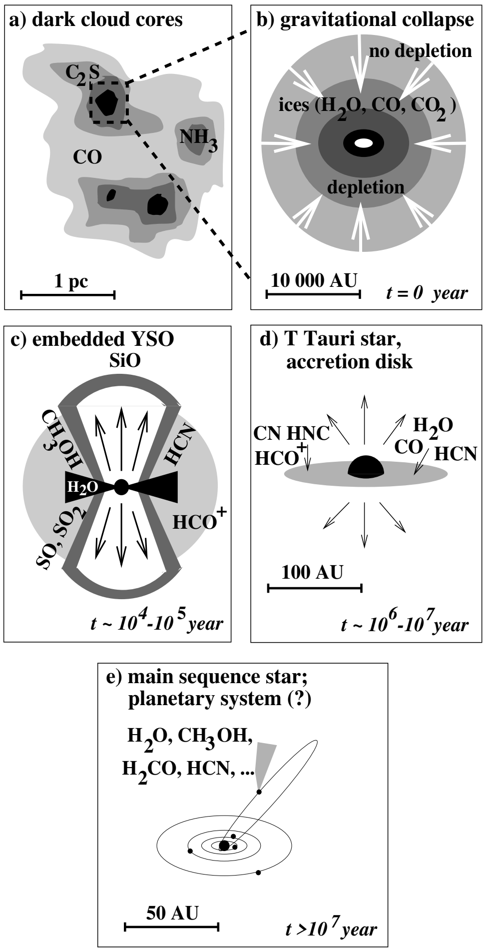

Figure 1. A schematic view of the characteristic molecules at different stages of low-mass star formation. (a) Dark cloud cores, where radicals and unsaturated carbon chains are prominent; (b) Collapse stage, where high levels of depletion of molecules have been inferred; (c) Deeply embedded YSO phase, where heating and supersonic outflows result in evaporation of ices and create a variety of chemical environments; (d) Young T Tauri star with a residual protoplanetary accretion disk containing gas-phase molecules and ices; (e) Mature planetary system with icy bodies such as comets (Figure by M.R. Hogerheijde, after Shu et al. 1987; from: van Dishoeck & Blake 1998).

envelopes around YSOs more directly on scales of $\sim 2''$–$20''$ (300–3000 AU at 150 pc) (Blake 1997) (see Figure 2).

Although much effort has focused on gas-phase chemistry, water ice was identified already in 1973 through its vibrational absorption toward bright infrared sources. The enormous advances in infrared instrumentation in the last decade, both from the ground and from space with the *Infrared Space Observatory* (ISO), have resulted in the detection of several other solid-state species and allow a complete inventory to be made (Tielens & Whittet 1997). The development of realistic models which include both gas-phase and grain-surface chemistry provides a challenge to theorists.

The combination of new observations and models has lead to the following scenario for the chemistry during star formation (see Figure 1). In the cold molecular cores prior to star formation, the chemistry is dominated by low-temperature gas-phase reactions leading to the enhanced formation of small radicals and unsaturated molecules. Long carbon-chains are produced if the gas is initially atomic-carbon rich. During the cold pre-stellar and collapse phases, many molecules accrete onto the grains and form an icy mantle. Here surface chemistry and processing by ultraviolet photons, X-rays and cosmic rays can modify the composition. Once the new star starts to warm the surrounding envelope, the ices are heated and molecules evaporate back into the gas phase, probably in a sequence according to their sublimation temperatures. In addition, the outflows from the young star penetrate the envelope, creating high temperature shocks and lower temperature turbulent regions in which both volatile and refractory material containing silicon can be returned. These freshly evaporated molecules then drive a rich chemistry in the 'hot cores' for a period of 10^5 yr. Finally, the envelope is dispersed by winds and/or ultraviolet photons, leading to the appearance of photon-dominated regions.

Part of the gas-phase and icy material is incorporated into the circumstellar disks, where they survive for a few $\times 10^6$ yr before being dispersed or assembled into new planetary bodies. Indeed, the connection between interstellar chemistry and solar system material has been greatly strengthened by observations of comets Hyakutake and Hale–Bopp, which reveal a remarkable similarity between the composition of interstellar and cometary ices (e.g., Ehrenfreund et al. 1997, Irvine et al. 1999).

Molecular spectroscopy is also a very powerful tool to probe the enormous range in temperatures from 10 to 10,000 K and densities from 10^4 to 10^{13} cm^{-3} that accompany the star-formation process. In addition, molecular lines provide the only means to trace the velocity fields in the highly-extincted circumstellar environment. In fact, the two analyses go hand in hand. On the one hand, an accurate physical model is a prerequisite for deriving reliable molecular abundances. On the other hand, it is important to know which molecule traces which physical component if its emission is to be used as a probe of the physical parameters.

This chapter first discusses the basic physical and chemical processes that play a role during star formation. Subsequently, the observational methods and problems in deriving of abundances are discussed. Finally,

Table 1 Identified interstellar and circumstellar molecules

Simple Hydrides, Oxides, Sulfides, Halogens and related molecules				
H_2 (IR)	CO	NH_3	CS	NaCl*
HCl	SiO	SiH_4^* (IR)	SiS	AlCl*
H_2O	SO_2	C_2 (IR)	H_2S	KCl*
N_2O	OCS	CH_4 (IR)	PN	AlF*
HF				
Nitriles and Acetylene derivatives				
C_3 (IR,UV)	HCN	CH_3CN	HNC	$C_2H_4^*$ (IR)
C_5^* (IR)	HC_3N	CH_3C_3N	HNCO	C_2H_2 (IR)
C_3O	HC_5N	CH_3C_5N ?	HNCS	
C_3S	HC_7N	CH_3C_2H	HNCCC	
C_4Si*	HC_9N	CH_3C_4H	CH_3NC	
	$HC_{11}N$	CH_3CH_2CN	HCCNC	
	HC_2CHO	CH_2CHCN		
Aldehydes, Alcohols, Ethers, Ketones, Amides and related molecules				
H_2CO	CH_3OH	HCOOH	CH_2NH	CH_2CC
H_2CS	CH_3CH_2OH	$HCOOCH_3$	CH_3NH_2	CH_2CCC
CH_3CHO	CH_3SH	$(CH_3)_2O$	NH_2CN	
NH_2CHO	$(CH_3)_2CO$	H_2CCO	CH_3COOH	
Cyclic Molecules				
C_3H_2	SiC_2	c-C_3H	CH_2OCH_2	
Molecular Ions				
CH^+ (VIS)	HCO^+	$HCNH^+$	H_3O^+	HN_2^+
HCS^+	$HOCO^+$	HC_3NH^+	HOC^+	H_3^+ (IR)
CO^+	H_2COH^+	SO^+		
Radicals				
OH	C_2H	CN	C_2O	C_2S
CH	C_3H	C_3N	NO	NS
CH_2	C_4H	HCCN*	SO	SiC*
NH (UV)	C_5H	CH_2CN	HCO	SiN*
NH_2	C_6H	CH_2N	MgNC	CP*
HNO	C_7H	NaCN	MgCN	
C_6H_2	C_8H	C_5N*		

From Ohishi (1997) with detections as of October 1998 added; Species denoted with $*$ have only been detected in the circumstellar envelope of carbon–rich stars. Most molecules have been detected at radio and millimeter wavelengths, unless otherwise indicated (IR, VIS or UV).

recent results on observations and models of the chemistry in the various star-formation phases are presented. This discussion focuses on those species whose abundances are particularly enhanced or decreased at a certain phase. These species often have only minor abundances in terms of overall composition —less than 10^{-7} with respect of hydrogen—, but provide important 'signposts' or 'clocks' of the evolutionary state of an object. This chapter is based on the recent reviews by van Dishoeck (1998a) on

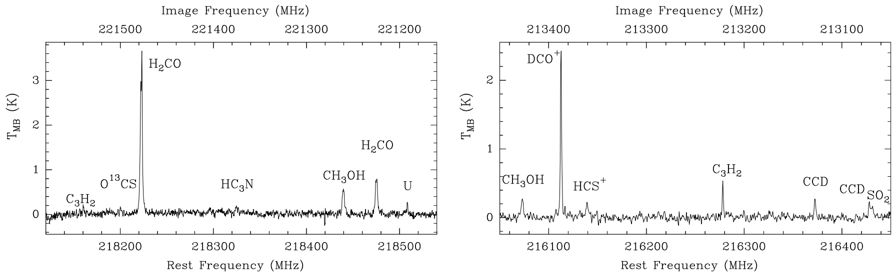

Figure 2. JCMT submilllimeter spectra of the deeply embedded low-mass YSO IRAS 16293−2422, showing lines of characteristic molecules such as H_2CO, CH_3OH and deuterated species (from: van Dishoeck et al. 1995).

the chemistry in diffuse and dense clouds, and by van Dishoeck & Blake (1998), van Dishoeck (1998b) and Langer et al. (1999) on the chemistry in star-forming regions. Other reviews on this subject include Hartquist et al. (1998), Irvine (1998) and van Dishoeck et al. (1993). For an excellent overview of the physics of molecular clouds, see Genzel (1992).

2. Gas-phase chemistry

2.1. BASIC MOLECULAR PROCESSES

The networks developed to describe the gas-phase chemistry in star-forming regions contain thousands of reactions between several hundreds of species (Millar et al. 1997a, Lee et al. 1996a). These thousands of reactions involve only a handful of different basic molecular processes, however, which have been described in detail in reviews by Dalgarno (1987) and van Dishoeck (1988). At the low densities in the interstellar gas, three-body processes are unimportant, so that only two-body reactions need to be considered. The rate of a reaction between species X and Y is given by $kn(\mathrm{X})n(\mathrm{Y})$ in cm^{-3} s^{-1}, where k is the reaction rate coefficient in cm^3 s^{-1} and n is the concentration in cm^{-3}.

There are two basic mechanisms by which molecular bonds can be formed (see Table 2). The first process is radiative association of gas-phase atoms or molecules, in which the new molecule is stabilized by the emission of a photon. The second mechanism is the formation of molecules on the surfaces of grains, in which the grain carries off the released energy corresponding to the molecular bond. The rate coefficients for the formation processes range from less than 10^{-17} up to 10^{-13} cm^3 s^{-1} and have considerable uncertainties, often up to an order of magnitude.

Molecules are readily destroyed by the absorption of ultraviolet pho-

TABLE 2. Some basic microscopic processes

Process	Name
Chemical Processes	
$X + Y \rightarrow XY + h\nu$	Radiative association
$X + Y{:}\mathrm{grain} \rightarrow XY + \mathrm{grain}$	Grain-surface formation
$XY + h\nu \rightarrow X + Y$	Photodissociation
$XY^+ + e \rightarrow X + Y$	Dissociative recombination
$X^+ + YZ \rightarrow XY^+ + Z$	Ion–molecule reaction
$X^+ + YZ \rightarrow X + YZ^+$	Charge–transfer reaction
$X + YZ \rightarrow XY + Z$	Neutral–neutral reaction
Heating and Cooling Processes	
grain or PAH + $h\nu \rightarrow$ grain$^+$ or PAH$^+$ + e^*	Photoelectric heating
H_2 + cosmic ray $\rightarrow H_2^+ + e^*$	Cosmic ray heating
$CO(J)$ + coll. $\rightarrow CO(J^*) \rightarrow CO(J') + h\nu$	CO line cooling
$O(^3P_2)$ + coll. $\rightarrow O(^3P_1) \rightarrow O(^3P_2) + h\nu$	[O I] line cooling
$C^+(^2P_{1/2})$ + coll. $\rightarrow C^+(^2P_{3/2}) \rightarrow C^+(^2P_{1/2}) + h\nu$	[C II] line cooling
gas + grain $\rightarrow$ gas$'$ + grain$'$	Gas–grain heating or cooling

tons. This process is very effective at the edges of dark clouds and in clouds located close to young stars (so-called photon-dominated regions (PDRs), Hollenbach & Tielens 1997, 1999). For molecules such as H_2 and CO, the photodissociation can take place only at very short wavelengths between 912 and 1100 Å, whereas most other species are dissociated by radiation out to 3000 Å. The ultraviolet photons can also ionize atoms with ionization potentials less than 13.6 eV (e.g., C, S, Si, Fe, Mg, ...), thereby increasing the electron abundance inside the cloud. In the unshielded interstellar radiation field such as given by Draine (1978), typical rates are 10^{-9}–10^{-10} s^{-1}, corresponding to lifetimes against photodissociation or photoionization of only 10^2–10^3 yr.

Inside a cloud, the ultraviolet radiation is reduced because of absorption and scattering by grains (e.g., Roberge et al. 1991). Deep inside dark clouds (>5 mag), little of the ambient radiation penetrates, but a weak ultraviolet field is maintained by cosmic-ray induced photons, resulting from the excitation of H_2 by secondary electrons produced by cosmic ray ionization of H_2 (Gredel et al. 1989). For a typical cosmic ray ionization rate ζ of a few $\times 10^{-17}$ s^{-1}, the resulting photorates are four to five orders of magnitude lower than those in the unshielded interstellar radiation field at the edge.

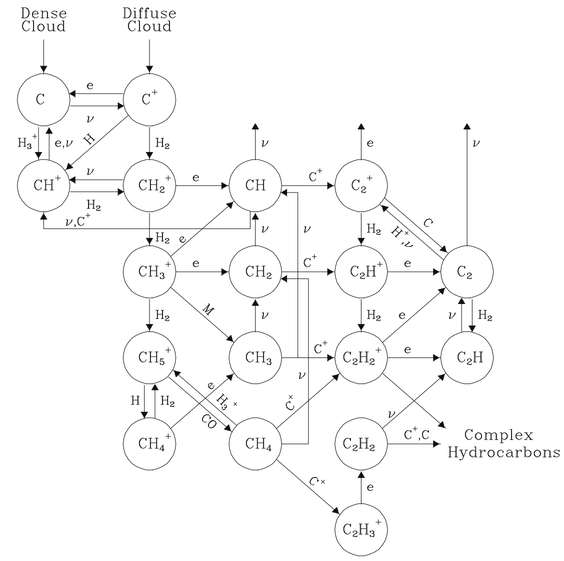

Figure 3. Initial steps in the gas-phase carbon chemistry in diffuse and dark clouds.

Molecular ions are efficiently destroyed by the process of dissociative recombination. Rate coefficients in 10–30 K gas are typically 10^{-7} to 10^{-6} cm^3 s^{-1}, with the lower values representative for H_3^+ —a key species in the chemistry (Dalgarno 1994, Larsson 1997). A major uncertainty in the models is the branching ratio to the various products. Complete experimental data are only just becoming available, and recent results indicate that three-body product channels (e.g., $H_3O^+ + e \rightarrow OH + H + H$ or $O + H_2 + H$) have a much larger probability than thought previously (e.g., Vejby-Christensen et al. 1997).

In dense clouds, destruction of neutral molecules can also occur through chemical reactions, in particular with He$^+$ (e.g., $He^+ + CO \rightarrow He + C^+ + O$). Collisional dissociation is only important in regions of very high temperature (> 3000 K) and density, such as found in shocks.

Once molecular bonds have been formed, they can be rearranged by chemical reactions leading to more complex species. The first generation of models (e.g., Herbst & Klemperer 1973, Prasad & Huntress 1980) included primarily ion-molecule reactions. The majority of these reactions are known to be fast at low temperatures owing to the long-range attraction between the ion and the molecule. It has recently been realized that neutral–neutral reactions involving radicals and/or atoms can also have rate coefficients as large as $\sim 10^{-10}$–10^{-9} cm^3 s^{-1} at low temperatures (e.g., Smith 1997, Kaiser et al. 1997).

2.2. GAS-PHASE NETWORKS

The gas-phase chemical networks describing the most important formation routes of various molecules based on the above processes have been discussed extensively in the literature, see reviews by, e.g., Millar (1990), Herbst (1995) and van Dishoeck (1998a). The abundances of the elements play a key role in the chemistry, especially the absolute and relative amounts of gas-phase carbon and oxygen in atomic or molecular form. It has recently become clear that the interstellar abundances of most elements are $\sim 30\%$ lower than the solar abundances (see Meyer 1997 for an overview). The fraction of heavy elements in the gas phase is large (at least 30%) in diffuse clouds, except for the most refractory elements (Si, Fe, ..), which are 99% in solid form. For dense clouds, the depletions of species like C, N, O and S are expected to be more significant, but are ill constrained observationally.

Because hydrogen is so much more abundant than any other element, reactions with H and H_2 dominate the networks if they are exothermic. This is only the case for small ions at low temperatures; most reactions of neutrals and large ions with H or H_2 have substantial barriers. H_2 itself is produced predominantly on the surfaces of grains (Hollenbach & Salpeter 1971), but once formed it is essential for the gas-phase chemistry of other species. Ionization of H_2 by cosmic rays at a rate ζ leads to H_2^+, which reacts with H_2 to form the stable H_3^+ ion. This ion plays a pivotal role in the subsequent ion-molecule chemistry through proton transfer. Its recent detection in interstellar space provides strong observational support for the gas-phase chemical networks (Geballe & Oka 1996, McCall et al. 1998).

The production of complex hydrocarbons in dense clouds occurs via three types of pathways (Herbst 1995): (i) carbon insertion reactions (e.g. $C^+ + CH_4 \rightarrow C_2H_2^+ + H_2$ or $C + C_2H_2 \rightarrow C_3H + H$); (ii) condensation reactions (e.g. $CH_3^+ + CH_4 \rightarrow C_2H_5^+ + H_2$ or $C_2H + C_2H_2 \rightarrow C_4H_2 + H$); and (iii) radiative association reactions (e.g. $C^+ + C_n \rightarrow C_{n+1}^+ + h\nu$) (see also Figure 3). In general, carbon insertion with C^+ is thought to be the dominant route. Since this leads to loss of one hydrogen and because the larger ions $C_nH_m^+$ do not react rapidly with H_2, low-temperature gas-phase chemistry produces strongly unsaturated hydrocarbons, in agreement with observations of dark clouds. The necessary C^+ ions are produced in small amounts through destruction of CO by He^+. Reactions with C may be competitive if they are as rapid as suggested by recent laboratory experiments. Once carbon is locked up in the very stable CO molecule, the formation of more complex hydrocarbons ceases.

At high temperatures of $\sim$ 200–2000 K such as encountered in the 'hot core' regions surrounding massive young stars and in shocks, gas-phase reactions with H and H_2 become significant. Specifically, the reactions O +

$H_2 \rightarrow OH + H - 4480$ K and $OH + H_2 \rightarrow H_2O + H - 2100$ K start to proceed at temperatures of a few hundred K (Ceccarelli et al. 1996, Charnley 1997), and drive most of the available gas-phase oxygen not locked up in CO into H_2O. Similar reactions of S with H_2 convert the gas-phase sulfur into H_2S. However, the back reactions of OH and H_2O with H have comparable energy barriers, so that the balance between O, OH and H_2O depends also on the H/H_2 ratio in the warm gas.

When most of the oxygen has been driven into H_2O at high temperatures, little O, OH and O_2 are available in the gas, preventing the formation of, for example, SO_2. Since O and O_2 also destroy reactive species such as CN, the CN abundance is enhanced at higher temperatures leading to enhanced formation of HC_3N through reaction with C_2H_2.

2.3. GAS-PHASE MODELS

2.3.1. *Depth-dependent vs. time-dependent models*

The calculation of the abundances in star-forming regions requires a physical model in which the temperature, density, radiation field etc. are specified as functions of position and/or time. In general, two different classes of models are considered: (i) Steady-state, depth-dependent models, in which the physical parameters and molecular abundances do not change with time, but are functions of depth into the cloud. Models of the translucent outer envelopes of clouds (e.g., van Dishoeck 1998a) and of dense ultraviolet photon- or X-ray dominated regions (PDRs or XDRs, see e.g., Hollenbach & Tielens 1997, Sternberg et al. 1997, Maloney et al. 1996) fall in this category. (ii) Time-dependent, depth-independent models, in which the concentrations are computed as functions of time at a single position deep into the cloud. Models of dark pre-stellar cores (e.g., Lee et al. 1996a, Millar et al. 1997b), collapsing envelopes (e.g., Bergin & Langer 1997) and hot cores near massive young stars (e.g., Charnley et al. 1992) fall into this category. The time scale for reaching chemical equilibrium depends on the density, temperature and ionization fraction and is typically 10^5–10^7 yr.

In both cases, the parameters that enter the models are (1) the elemental abundances of C, O, N, S, metals...; and (2) the cosmic ray ionization rate ζ in s^{-1}. In the steady-state, depth-dependent models, additional parameters are (3) the geometry (e.g. plane-parallel, spherical, ...); (4) the density $n_H = n(H) + 2n(H_2)$ as a function of position; (5) the incident radiation field, specified by a factor I_{UV} times the standard interstellar radiation field as given by, e.g., Draine (1978); and (6) the grain parameters, i.e., the extinction curve, albedo and scattering function. The temperatures of the gas and dust as functions of position in the cloud can be obtained self-consistently from the balance of the heating and cooling processes listed in Table 2. Alternatively, they can be constrained from observations and provided as additional input parameters (see §4.2).

In the time-dependent models, the additional parameters besides (1) and (2) are: (3) the density, usually taken to be constant with time (so-called pseudo time-dependent models); (4) the visual extinction A_V at the position in the cloud, usually taken to be so large that external photons can be neglected; and (5) the initial abundances of the various species at t=0, often taken to be atomic except for H_2. The temperature can be obtained from the thermal balance, but is almost always set at 10 K for both the gas and dust, typical of a dark cloud shielded from ultraviolet radiation and heated by cosmic rays only. In comparison with observations, the ratios of the local concentrations (in cm^{-3}) are taken to be equal to the ratios of the column densities integrated over depth (in cm^{-2}). This assumption is accurate for molecules whose abundances peak in the center of the cloud, but not necessarily for species such as radicals whose abundances peak in the outer part of the envelope (see Figure 5 of van Dishoeck 1998a).

2.3.2. *The $C^+ \rightarrow C \rightarrow CO$ transition*

The principal chemical characteristics of the depth- and time-dependent models are governed by the transition of carbon from atomic to molecular form. In the depth-dependent case, C^+ recombines to C around $A_V \approx 1$ mag, followed by the conversion to CO around $A_V \approx 2$ mag. The CO photodissociation rate as a function of depth is crucial in this transition (e.g., van Dishoeck & Black 1988, Lee et al. 1996b). The chemistry of other species follows the $C^+ \rightarrow CO$ transition. At the edge, only the simplest diatomic molecules are found. Around $A_V = 1$–2 mag, the presence of both C and C^+ and simple hydrides results in an increase in the abundance of hydrocarbon molecules such as CN and C_2H. Deeper inside the cloud, atomic carbon is no longer available, and destruction by O becomes more important than photodissociation. Stable species such as CH_4, C_2H_2 and HCN become dominant.

Many of the same features are observed in the pseudo time-dependent models, if depth is replaced by time. These models usually start with the assumption that dark clouds originate from diffuse gas, so that all species except H_2 are initially in atomic form, with carbon present as C^+. On a time scale of $\sim 10^3$ yr, C^+ recombines to C, which subsequently transforms to CO after $\sim 10^5$ yr. Since the presence of atomic carbon is essential to build up more complex organic species such as HC_3N, they are abundant only at early times, but not at steady-state (see Figure 4).

The main time-dependent aspects of the other elemental pools —O, N and S—, depend on how their chemistry is linked to that of carbon. For example, the abundance of CS has a different time behavior than that of

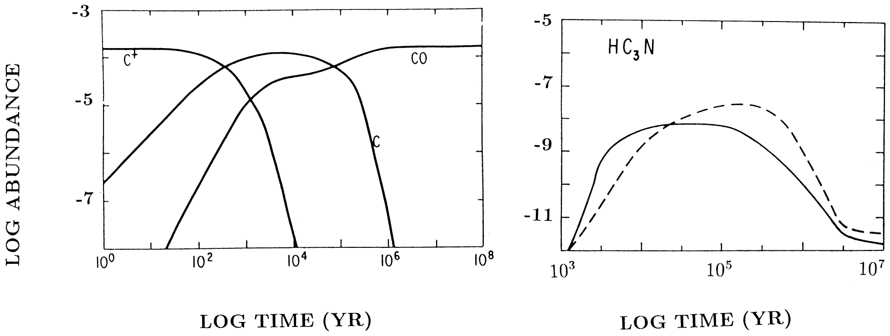

Figure 4. Time dependence of the abundances of C^+, C and CO (left) and HC_3N (right) for a cloud with $n_H = 2 \times 10^4$ cm^{-3}. The latter behavior is typical of all complex carbon–bearing molecules (from: Herbst & Leung 1986).

SO, because CS is formed by reactions with carbon-hydrides, whereas SO is destroyed by atomic carbon. This leads to two classes of molecules: (i) species like CN, HCN, CS and complex carbon chains, whose production is linked to the carbon network and which have larger abundances at early times; and (ii) molecules such as N_2, NH_3, N_2H^+ and SO that are independent or destructively linked to the carbon chemistry and which exhibit higher abundances at equilibrium.

2.4. FRACTIONATION

At the low temperatures of pre-stellar cores and the outer envelopes of YSOs, significant enhancement of minor isotopes can occur as a result of so-called 'fractionation'. The most relevant case for star-forming regions is the deuterium fractionation, initiated by the isotope exchange reactions H_3^+ + HD $\rightarrow$ H_2D^+ + H_2 and CH_3^+ + HD $\rightarrow$ CH_2D^+ + H_2 (Wootten 1987, Millar et al. 1989). These reactions occur preferentially in the forward direction at low temperatures, because the heavier H_2D^+ and CH_2D^+ are slightly more stable than H_3^+ and CH_3^+ due to their lower zero-point vibrational energy. H_2D^+ and CH_2D^+ subsequently transfer the deuterium to, for example, CO or N to form DCO^+ or $DCNH^+$. The latter ion leads to DCN through dissociative recombination. The observed DCO^+/HCO^+ and DCN/HCN abundance ratios are factors of 100 to >1000 larger than the overall [D]/[H] ratio of $\sim 1.6 \times 10^{-5}$.

2.5. SUCCESSES AND PROBLEMS

Pure gas-phase chemistry models have been remarkably successful in explaining many observed features of interstellar chemistry (Herbst 1995, Turner et al. 1998). These include the abundances of simple species in diffuse and translucent clouds; the presence of H_3^+ and the related high abundances of protonated species such as HCO^+ and N_2H^+ in dark clouds; the high abundances of unsaturated and metastable molecules in dark clouds such as $l-$ and $c-C_3H$ or HNC; and the large isotopic fractionation.

Most of the problems with gas-phase models stem from uncertainties in the basic reaction rates. For example, if reactions of bare carbon chains C_n with O or N are rapid, the observed abundances of carbon-chain molecules like HC_7N cannot be reproduced, even at early times. Another complication is that time-dependent models have more than one solution in certain regions of parameter space (e.g., le Bourlot et al. 1995, Lee et al. 1998). It is not yet clear, however, what the astrophysical consequences of this 'bistability' phenomenon are. Finally, gas-phase models of dark clouds predict that a substantial fraction of the oxygen is driven into O_2 at low temperatures. Recent limits on the O_2/CO ratio of less than 0.03 are difficult to accomodate in such models (Olofsson et al. 1998, Marechal et al. 1997, Melnick et al. 1998).

3. Grain-surface chemistry

3.1. BASIC SURFACE PROCESSES

The chemistry on the surfaces of interstellar grains has received ample discussion in the literature (e.g., Tielens & Allamandola 1987, Herbst 1993, Tielens & Charnley 1997, Langer et al. 1999). Four different steps can be distinguished: (i) accretion; (ii) diffusion; (iii) reaction; and (iv) ejection or evaporation. The time scale for a molecule to collide with a grain and accrete is given by $t_{\rm acc} \approx 2\times10^9/n_{\rm H}y_S$ yr where y_S is the sticking probability which is thought to lie between 0.1 and 1.0 for most species (see Williams 1993 for a review). Thus, in envelopes around YSOs with densities of order 10^5 cm^{-3} or larger, the time scale for depletion is shorter than the collapse time (Walmsley 1991). The timescales for diffusion and evaporation increase exponentially with the binding energies of the species to the grain, which in turn scale with its mass in the case of physical adsorption. Under most interstellar circumstances, the rate-limiting step is the accretion of new species rather than the diffusion over the surface.

Because atomic hydrogen is so abundant and mobile, grain-surface chemistry leads primarily to hydrogenated species such as H_2O, NH_3 and CH_4. Although many of the surface reactions have energy barriers, they can still

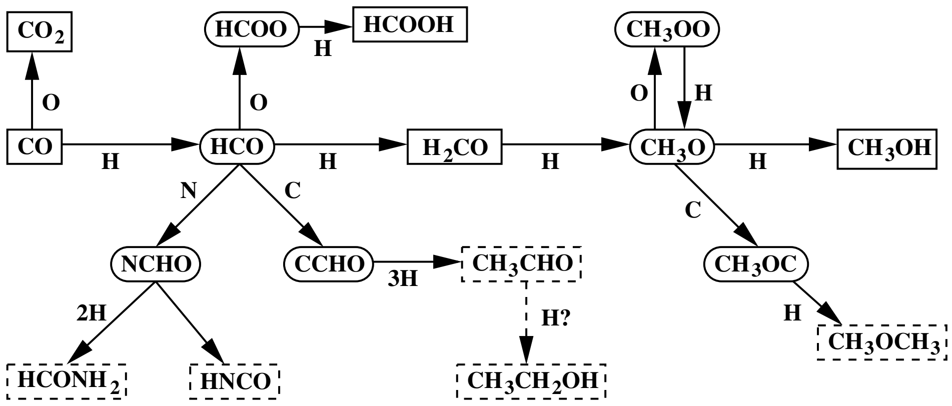

Figure 5. Grain-surface chemistry routes involving CO. Solid rectangular boxes contain molecules which have been identified in interstellar ices, whereas dashed boxes indicate molecules detected in the gas phase in hot cores (figure by Tielens, based on Tielens & Hagen 1982).

proceed because of the relatively long time scale ($\sim$ 1 day) available for reaction before another species is delivered from the gas to the grain.

The dominant molecule accreted from the gas is CO, and it therefore forms a key in the surface chemistry. Hydrogenation of CO leads to HCO, H_2CO and eventually CH_3OH (see Figure 5). The intermediate HCO (formyl) and CH_3OH (methoxy) radicals can also react with various other accreted species, leading to more complex organic molecules such as CH_3CHO, HCOOH and $HCONH_2$. The identification of many of these species in molecular clouds, directly in ices or indirectly in hot cores where the ices have evaporated off the grains, provides support for this scheme.

Hydrogenation of molecules is particularly effective in the outer regions of YSO envelopes where the atomic hydrogen abundance is high. At densities greater than $\sim 10^5$ cm^{-3} shielded from ultraviolet radiation, atomic oxygen becomes more abundant than atomic hydrogen, leading to oxidation of various accreted molecules. For example, CO can react with O to form CO_2, and O_2 with O leads to O_3.

Deuterium fractionation of molecules can also occur through grain-surface chemistry, because the gas-phase atomic D concentration inside dense clouds is enhanced compared with atomic H through dissociative recombination of DCO^+ (Tielens 1983). The atomic D can then react with molecules on the surface to form deuterated species. Doubly-deuterated molecules such as D_2CO and NHD_2, which have been detected in the envelopes around low- and high-mass stars, are thought to be formed by this route (e.g., Ceccarelli et al. 1998).

TABLE 3. Interstellar ice composition and evaporation temperatures

Species	Abundance[a]	T_{ev}[b] (K)
H_2O	100	90
CO	16	16
CO_2	24	50
CH_4	2	18
CH_3OH	4	80
XCN	2	?
OCS	...	85
NH_3	10[c]	55
N_2	...	13
O_2	< 30[d]	13

[a] Abundances are relative to H_2O=100, and refer to NGC 7538 IRS9 (Whittet et al. 1996). Abundances are variable from source to source due to differential outgassing and thermal processing. The H_2O abundance is typically 10^{-4} with respect to H_2.
[b] Evaporation temperatures for pure ices under interstellar conditions; see text for mixed ices.
[c] Tentative identification by Lacy et al. (1998).
[d] Vandenbussche et al. (1999).

3.2. THERMAL PROCESSING AND EVAPORATION

In star-forming regions, the ice mantles formed in the cold pre-stellar and collapse phases can be heated by the young star. This leads to restructuring of the ice matrix and outgassing when the temperature is near its sublimation point. Table 3 summarizes the sublimation temperatures of various species under interstellar conditions (Sandford & Allamandola 1990, 1993); these are typically lower than found in laboratory experiments because of the lower pressures in space. Interstellar ices are not pure, but in mixed ices, the evaporation of each component is largely determined by its own sublimation behavior, unless the abundance of one of the species is less than $\sim$ 5%. Thus, an ice mixture of $H_2O/CO/CO_2$=2/1/1 shows release of CO around 20 K, CO_2 around 50 K and H_2O around 90 K. However, a mixture of H_2O/CH_4=100/1 shows evaporation of both H_2O and CH_4 around 90 K. Only a small fraction of the CO or CO_2 stays behind, and is released when the whole H_2O ice rearranges from amorphous to crystalline form.

Ices containing CH_3OH show particularly interesting behavior upon heating, because CH_3OH has a sublimation temperature above that of the phase transformation of H_2O. Thus, H_2O/CH_3OH ices heated to $\sim$ 80–

90 K will segregate into rather pure H_2O- and CH_3OH domains (Blake et al. 1991). Recent experiments indicate that CO_2/CH_3OH mixtures show similar segregation behavior (Ehrenfreund et al. 1998), and evidence for this process is seen in the observed profiles of interstellar solid CO_2 toward massive YSOs (Boogert et al. 1999, Gerakines et al. 1999).

3.3. NON-THERMAL DESORPTION

Thermal evaporation is only efficient at dust temperatures $T_{\rm dust}$ higher than 20 K. Some desorption can also occur by non-thermal processes in the cold pre-stellar cores and outer envelopes with $T_{\rm dust} \approx 10$ K. These processes have been reviewed most recently by Schutte (1996), and include cosmic ray spot heating, heating due to the energy liberated by the formation of molecules on grains, heating due to grain–grain collisions, and explosive heating due to exothermic reactions between stored radicals on grains. The desorption time scales depend strongly on the binding energies of the molecules at the surfaces and the surfaces involved (silicates, carbonaceous material, ices). All of them are particularly effective for non-polar ices containing CO, O_2 and N_2, and less for H_2O-rich ices which contain strong hydrogen bonds.

3.4. ENERGETIC PROCESSING

The cosmic-ray induced ultraviolet photons and the radiation produced by the young star can further process the ices. Ultraviolet photolysis of H_2O, CO, NH_3 and CH_4 produces radicals which can react with each other and with the parent molecules to form more complex molecules like H_2CO, HCOOH and $HCOCH_3$ (e.g., Bernstein et al. 1995, Gerakines et al. 1996). Much of the outcome of this chemistry is very similar to that of the hydrogenation of CO, and further quantitative studies are needed to assess their relative importance.

Photolysis of ice mixtures containing H_2O, CO, NH_3 and CH_3OH often leaves a non-volatile organic residue containing a variety of complex molecules (e.g., Schutte et al. 1993, Bernstein et al. 1995). Some of these chemical effects are also found in experiments in which ices are bombarded with highly-energetic charged particles, analogous to cosmic rays or X-rays (e.g., Moore et al. 1983, Kaiser & Roessler 1997, Teixeira et al. 1998). The photochemical and high-energy bombardment processes are often referred to as 'energetic' processing in the literature, without discrimination.

3.5. POLAR AND APOLAR ICES

The ices in interstellar clouds are generally not homogeneous, but consist of different layers or domains (e.g., Tielens et al. 1991, Ehrenfreund et al. 1998). Two broad classes of ices can be distinguished. Polar ices are dominated by H_2O ice and contain minor amounts of CO_2, CO, CH_4 and CH_3OH. Apolar ices are dominated by species such as CO and perhaps some O_2 and N_2, but contain very little H_2O. The two phases can be distinguished by their line profiles, since the force constants of CO molecules embedded in an H_2O-matrix will be slightly different from those of CO surrounded by other CO molecules.

The different ice phases can arise from a combination of at least two processes, caused by the density and temperature gradient in YSO envelopes (see Schutte 1999 for review). First, the density gradient results in a steep gradient in the gas-phase H/CO ratio. At low densities or at the edge of the cloud, the high concentration of H results in polar ices. Deep inside the envelope at high densities, mostly apolar ices of accreted CO, O_2 and N_2 form. Layered ices can be produced in a collapsing envelope with the polar ices condensing first and the non-polar species forming a volatile 'crust'. Second, the evaporation processes can shape the composition of the ice mantles, because the desorption mechanisms are much more efficient for volatile non-polar species like CO than for non-volatile material like H_2O and CH_3OH. This 'distillation' effect decreases the apolar ices compared with the polar ices at higher temperatures.

3.6. GAS–GRAIN MODELS

Based on the above processes, two different chemical regimes can be distinguished in models which take both gas-phase and grain-surface processes into account. In the 'accretion-limited' regime, the diffusion time is much shorter than the accretion time so that a species can diffuse on the surface until it finds a co-reactant. The chemistry is limited by rate at which new species are delivered to the surface. In the 'reaction-limited' regime, the opposite holds so that many reactive species are present on a grain surface and the reaction is controlled by surface concentrations as well as kinetic parameters. Most of the gas–grain chemical models have been formulated in the 'reaction-limited' regime using rate equations which mirror those used for gas-phase chemistry (e.g., Hasegawa & Herbst 1993). This approach is only accurate when a large number of reactive species exist on a single grain surface, since only average abundances are calculated. This condition is usually not met in interstellar clouds, since the accretion times are long, grains are small, and reactions are fast, so that at most one reactive species is present on a grain at any time. The surface chemistry is therefore in the accretion-limited regime and can only be properly treated by a Monte-Carlo method which determines the likelihood of two such species arriving from the gas in succession onto a particular grain in a steady-state model (e.g., Tielens & Hagen 1982). Recently, ad-hoc modifications of the rate equations have been proposed to correct the shortcomings of the reaction-limited approach (Caselli et al. 1998, Shalabiea et al. 1998).

3.7. SUCCESSES AND PROBLEMS

The observations of H_2 in diffuse clouds and of large amounts of ices in dense clouds can only be explained in models in which these molecules are formed on the surfaces of interstellar grains and/or accreted from the gas. Thus, gas–grain interactions play an essential role in interstellar chemistry. The main problem is an accurate, quantitative description. Many basic grain-surface reactions with H or O at low temperatures are still poorly understood theoretically or ill-constrained by laboratory experiments, partly because the details of the surfaces of interstellar grains are still poorly characterized.

4. Determination of molecular abundances

The comparison of observations and chemical model calculations ultimately depends on the translation of spectral-line data into molecular abundances. In the following, the observational techniques will be discussed, and the methods for constraining the physical structure and subsequently the chemical abundances will be outlined.

4.1. OBSERVATIONAL TECHNIQUES

The energy level structure of a molecule can be decomposed into an electronic part $E_{\mathrm{e}\ell}$, a component due to the vibrational motion of the nuclei E_{vib}, and a component describing the overall rotation of the molecule in space E_{rot}. In general, $E_{\mathrm{e}\ell} >> E_{\mathrm{vib}} >> E_{\mathrm{rot}}$: transitions between two electronic levels lie typically in the visible/ultraviolet part of the spectrum, those between two vibrational levels in the infrared part, and those between two rotational levels at (sub-)millimeter wavelengths. Because of the high extinction, only infrared and millimeter observations are feasible in star-forming regions.

4.1.1. *Rotational line emission at (sub-)millimeter wavelengths*

Most molecules listed in Table 1 are observed by their rotational transitions within the ground electronic and vibrational state (Figure 6). The sensitivity of large single-dish (sub-)millimeter telescopes allows the detection of

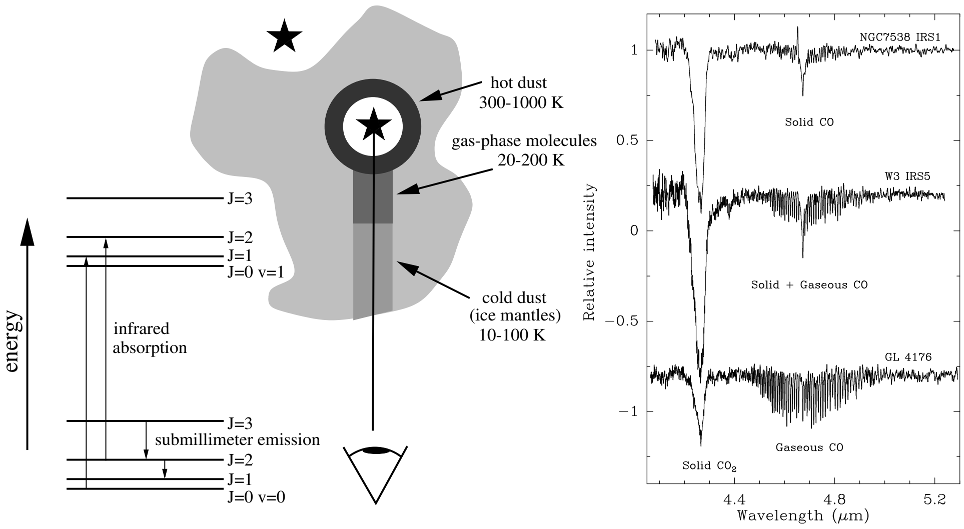

Figure 6. Left: Schematic illustration of infrared absorption line observations of gas and dust toward embedded or background sources. The infrared continuum is provided by the hot dust at 300–1000 K. Right: Normalized ISO–SWS spectra toward three massive young stellar objects embedded in dense molecular clouds. The strong, broad absorption at 4.27 μm is due to solid CO_2, whereas the characteristic ro-vibrational P- and R-branch structure at 4.4–4.9 μm indicates the presence of warm, gaseous CO along the line of sight (van Dishoeck et al. 1998).

weak lines and rare chemical species and isotopes down to abundances of 10^{-11} with respect to hydrogen. However, not all molecules can be observed by this method. Symmetric molecules lack the permanent dipole moment required for rotational emission lines, so that important species like H_2, N_2, CH_4 and C_2H_2 cannot be observed in this way. In addition, the Earth's atmosphere prevents ground-based observations of low-lying transitions of O_2, CO_2 and H_2O. Because of its chemical stability, CO often serves as a tracer of H_2, assuming either a fiducial CO/H_2 abundance ratio or a conversion factor between integrated CO intensity and H_2 column density (see van Dishoeck & Black 1987, van Dishoeck 1998a for reviews). The only direct measurement of $CO/H_2 = 2.7 \times 10^{-4}$ in the warm dense cloud toward NGC 2024 IRS2 (Lacy et al. 1994) is a factor of 3 higher than the value of 8×10^{-5} commonly used in dark clouds (Frerking et al. 1982). Submillimeter continuum emission from dust can also act as a standard when values are adopted for the dust emissivity, its temperature, and the dust-to-gas mass ratio.

Clouds can be mapped at angular resolutions between $10''$ (1500 AU at 150 pc) and a few arcminutes with single-dish instruments. Even in the nearest star-forming clouds, regions of different physical or chemical characteristics (envelope, outflow, disk, ...) are likely to fall within one beam, complicating the derivation of molecular abundances. Much higher angular resolution of the order of one arcsecond is offered by interferometers. However, the sensitivity of these instruments is lower than that of single-dish telescopes, and their interpretation is complicated because they filter out all emission on extended scales defined by the shortest baselines (cf. §8.1).

A major advantage of heterodyne (sub-)millimeter spectroscopy is the very high spectral resolution, typically better than a few tenths of a km s^{-1} and covering the full extent of the lines up to a few hundred km s^{-1}. This allows separation of regions with different physical conditions within one beam if they have different velocities or line profiles. A drawback of rotational emission spectroscopy is that the frequency separation between different transitions of the same molecule is usually too large to be obtained in a single setting, and multiple observations are needed to constrain the excitation, often involving different telescopes or beam sizes.

4.1.2. *Vibrational absorption at infrared wavelengths*

Absorption of infrared emission into (ro-)vibrationally excited levels of molecules offers a complementary view of the chemical content (see Figure 6). Background stars or embedded objects of sufficient infrared brightness can usually be found in star-forming regions, often the YSO under study itself. Absorption lines probe molecular gas along a pencil beam to the infrared source with very high angular resolution, but mapping is not possible and different conditions still exist along the line of sight. The velocity resolution is generally lower, so that the line profiles are often not resolved.

Because of the low spectral resolution and the intrinsic strengths of the transitions, the abundance limit of infrared observations is two to four orders of magnitude higher than that at millimeter wavelengths. On the other hand, symmetric species like C_2H_2 and CH_4 can be observed, because the vibrational modes induce a temporary dipole moment. Different transitions of a molecule often fall in a single infrared spectrum, providing direct constraints on the molecular excitation up to high energy levels. By their very nature, absorption lines also directly measure the line opacity, if the profiles are resolved. Another major advantage is that infrared studies are not limited to the gas phase. Molecules frozen onto dust grains show a markedly different line profile, since the rotational degrees of freedom are collapsed into a single, broad feature which is slightly shifted from the position of that of the gas-phase molecule (Figure 6). This offers the possibility to study the relative amounts of a species present in the gas-phase and in the condensed phase, and to probe the ice mantles as formation sites of various molecules like CH_3OH and H_2CO. The *Short Wavelength Spectrometer* (SWS) on ISO is particularly well suited for such studies (see §6.2, Figure 6 and 10).

4.2. CONSTRAINING THE PHYSICAL STRUCTURE

In order derive molecular column densities or abundances from the observations, a good physical model of the region is a prerequisite. Observations of different rotational lines provide very useful probes, because they are collisionally excited by H_2 for densities of 10^2–10^7 cm^{-3} and temperatures of 5–200 K (Evans 1980, Walmsley 1987, Genzel 1992).

The statistical equilibrium equations for the level populations n_i due to radiative and collisional processes are given by

$$n_i \sum_{j<i} A_{ij} + n_i \sum_j (B_{ij} J + C_{ij} n_{\rm col}) = \sum_{j>i} n_j A_{ji} + \sum_j n_j (B_{ji} J + C_{ji} n_{\rm col}),$$

where the left-hand side represents the processes leading to the loss of population of level i and the right-hand side the gain of population. Here A_{ij} and B_{ij} are the Einstein A and B coefficients for spontaneous and stimulated emission and absorption, J is the intensity of the radiation field averaged over all directions and integrated over the line profile, C_{ij} is the collisional rate coefficient between levels i and j, and $n_{\rm col}$ is the density of collision partners, primarily H_2. The upward and downward rate coefficients are related through detailed balance by $C_{ji} = (g_i/g_j) C_{ij} \exp(-h\nu/kT)$. The values of C_{ij} for collisions of different molecules with H_2 J=0 have largely been derived from detailed quantum mechanical calculations (Green 1975, Flower 1990), and form one of the largest uncertainty in analyzing molecular excitation. Information on collisional rate coefficients at high temperatures >200 K is still scarce, and collisions with H_2 J=1 or higher are generally not taken into account explicitly.

The critical density for a given transition is the density at which the rates for collisional processes become comparable to those for radiative processes, resulting in substantial population of level i. In formula, $n^i_{\rm crit} = A_{ij} / \sum_j C_{ij}$. If the transition becomes optically thick, the critical density is lowered by $1/\tau$, since part of the emitted photons are re-absorbed. Here τ is the optical depth of the line. Note that higher frequency transitions have higher critical densities, since $A_{ij} \propto \nu^3$. Also, molecules with large dipole moments μ have high critical densities, since $A_{ij} \propto \mu^2$. Thus, by choosing the appropriate molecule and transition, a large range of densities can be probed. This is schematically indicated in Figure 7, which shows the range of physical parameters for which different line ratios are most sensitive.

The contribution of the line photons to the excitation is taken into account by a variety of formalisms, including the large velocity gradient,

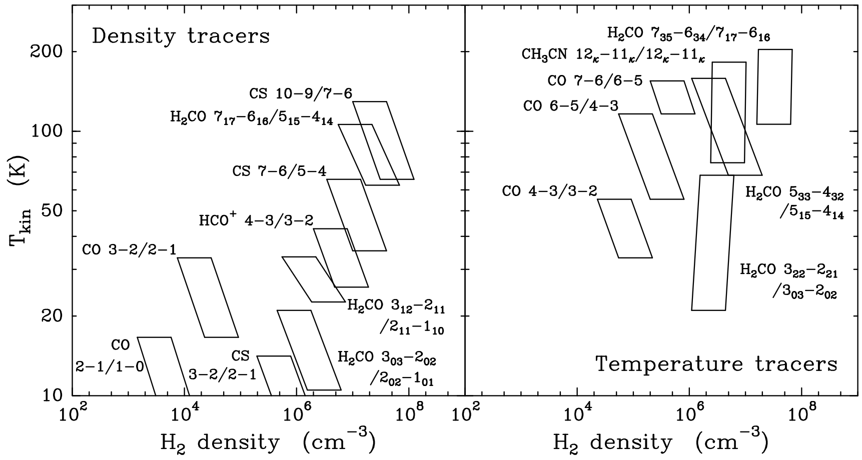

Figure 7. Examples of molecular line ratios which are used to constrain the density and temperature structure of YSO envelopes.

Sobolev, microturbulent, or escape probability methods (e.g., Sobolev 1960, Habing 1988, Osterbrock 1989 Appendix 2).

4.3. FROM OBSERVATIONS TO ABUNDANCES

Figure 8 gives a schematic overview of the steps involved in the determination of abundances from observations. Correcting for atmospheric effects and telescope losses yields the antenna temperature. This is the actual sky brightness averaged over the main forward beam of the telescope, or, for interferometric observations, the sky brightness averaged over the synthesized beam size after spatial filtering by the array baselines.

Relating the antenna temperature to the underlying brightness distribution on the sky requires assumptions about the source structure. Figure 8 illustrates two extreme approaches to this problem. The 'homogeneous' method, shown on the left, uses a single set of physical conditions and a given size, or beam-filling factor, for the source, which transforms the beam-averaged antenna temperature into brightness temperature on the sky. The molecular excitation and opacity relate this brightness temperature to the column density of the molecule. The line opacity follows from the intensity ratio of lines of different isotopic varieties. The excitation can either be assumed to be in local thermodynamic equilibrium, valid if the density exceeds the critical density for the observed transition, or can be derived from statistical equilibrium and radiative transfer calculations as described above once the physical parameters have been constrained. Repeating the procedure for an appropriate abundance standard like CO yields the molecular abundance relative to H_2.

More complex source structures can be described with multiple 'homogeneous' components, each with its own beam-filling factor. This approach works well if the number of different components is limited, for example, if the cloud is described as a collection of dense clumps embedded in a more diffuse interclump medium (e.g., Hogerheijde et al. 1995). When the beam is filled with a large number of different physical regimes, as is the case, e.g., for the power-law density and temperature distributions often used to describe YSO envelopes, the multi-component 'homogeneous' approach no longer suffices. The right-hand side of Figure 8 shows a more 'detailed' method. Starting with a fiducial source model, the molecular excitation and the radiative transfer throughout the cloud is calculated. Monte-Carlo techniques are often used in this step (e.g., Bernes 1979). The emergent sky brightness distribution is convolved with the telescope beam, or sampled at the interferometer's spatial frequencies. Matching the observed and model antenna temperature constrains the molecular abundance.

The interpretation of interferometric observations, and the derivation of molecular abundances from them, requires that spatial filtering by the interferometer is taken into account explicitly. Even if the data sets of the molecule in question and that of a standard like $C^{18}O$ contain the same spatial frequencies, both lines can have very different distributions of intensity over those frequencies if they trace different physical regimes. Different levels of flux are resolved out by the interferometer, resulting in abundance estimates deviating by factors of a few or more if not accounted for properly.

5. Chemistry in pre-stellar cores

In the following sections, an overview will be given of recent observations and models of star-forming regions at different evolutionary stages, using the material presented in §1-4 as general background information. The discussion focuses on those species whose abundances are most affected at a particular evolutionary state. These molecules are often only minor components in terms of the overall composition of the gas or dust. Recent overviews of the major reservoirs of the principal elements C, N and O are given, e.g., in van Dishoeck et al. (1993) and van Dishoeck & Blake (1998). In brief, most of the oxygen is contained in solid silicates, oxides and ices, as well as gas-phase O, CO and, in warm regions, H_2O. Most of the carbon is in some solid carbonaceous form, with the remainder in gas-phase CO. Nitrogen is mostly locked up in gas-phase N_2 and N, but the amount in

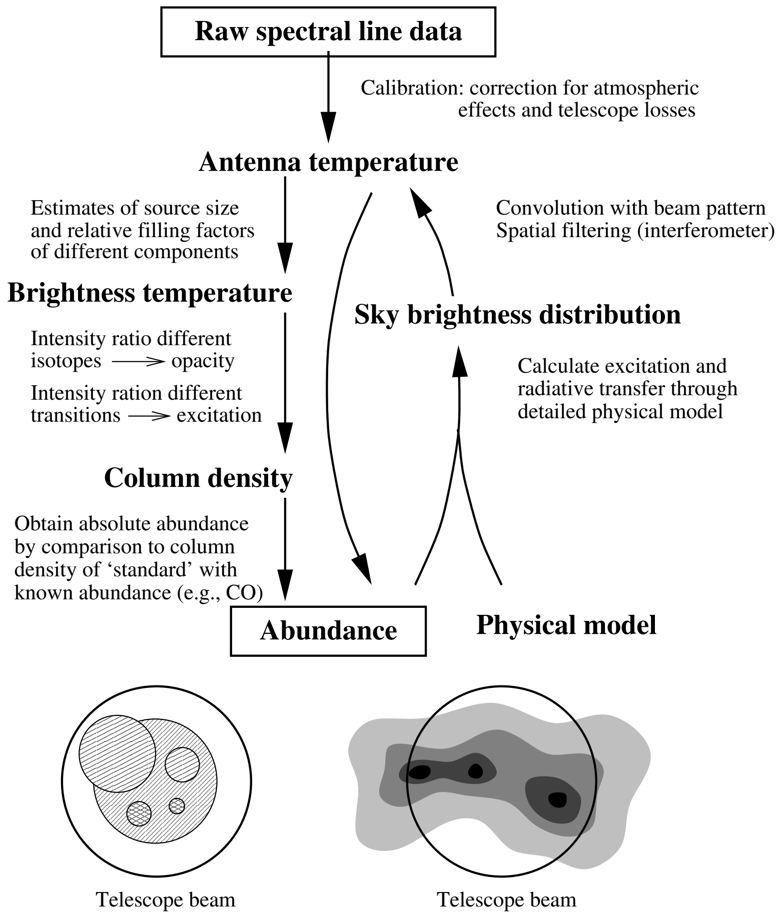

Figure 8. The steps involved in deriving molecular abundances from spectral line data. The left-hand side shows the 'homogeneous' approach, the right-hand side the 'detailed' approach.

solids is poorly constrained.

5.1. TRANSLUCENT CLOUDS

In order to study the effect of YSOs on the chemistry and test the basic chemical networks, the abundances in quiescent clouds prior to star formation need to be constrained. The best clouds for this purpose are the translucent and high-latitude clouds with visual extinctions of a few mag and densities of a few thousand cm^{-3}. These clouds have been studied by optical absorption lines against reddened stars (e.g., Gredel et al. 1993), by millimeter absorption lines against distant radio sources (e.g., Lucas & Liszt 1997) and by millimeter emission observations (e.g., Turner 1996, 1998 and references cited). No signs of star formation have been found in these regions. The chemistry is characterized by simple diatomic and triatomic molecules, radicals and ions. Detailed models by Turner et al. (1998) show that the observed abundances of most species are well reproduced by the ion-molecule networks. The main exceptions are formed by NH_3, H_2CO and H_2S, whose formation is probably dominated by grain-surface chemistry.

5.2. DARK CLOUD CORES

More than 100 dark cores have been identified through optical extinction and molecular line studies, at least half of which have not yet formed any stars (Myers & Benson 1983, see chapter by Myers). Most chemical studies have been directed toward TMC-1, a small elongated, dense ridge of $\sim 0.6 \times 0.06$ pc in Taurus with a mass of less than 40 $M_\odot$. This clump shows a particularly rich chemistry, with a large chemical gradient across the core. NH_3 and other 'late' molecules peak in the northern part, whereas long carbon-chain molecules such as HC_7N and C_4H are most abundant in the southern part (Olano et al. 1988, Pratap et al. 1997). High spectral and spatial resolution observations show that there are at least three different velocity components in this region on less than 10,000 AU scales, with different intensity ratios among the molecules (Langer et al. 1997). The abundances of the carbon-chains range from 10^{-11} up to 10^{-8} and are several orders of magnitude larger than found in other dark clouds. Such large abundances are usually interpreted with pseudo time-dependent models at 'early times' $t \approx 10^5$ yr, assuming that the cloud evolved from a diffuse cloud phase in which carbon was initially in atomic form (e.g., Lee et al. 1996a).

In order to investigate whether TMC-1 is chemically peculiar, Suzuki et al. (1992) and Benson et al. (1998) performed a systematic study of a few characteristic molecules (C_2S, HC_3N, HC_5N, N_2H^+ and NH_3) in a large set of dark cores. The abundances of the carbon chains are found to correlate well with each other, but not with NH_3 or N_2H^+, consistent with the case of TMC-1. The observed C_2S/NH_3 abundance has been reproduced quantitatively in models which start from diffuse gas and form dense cores over a period of 10^5 to 2×10^6 yr (see Figure 9). In this scenario, TMC-1S is one of the youngest clouds. There are numerous other non-equilibrium processes, however, such as penetration of ultraviolet radiation, outflows or turbulence, which can lead to the breakdown of CO into C or C^+ and therefore give the cloud core a chemically 'young' appearance. Thus, the 'chemical age' does not necessarily measure the true age of the core, but

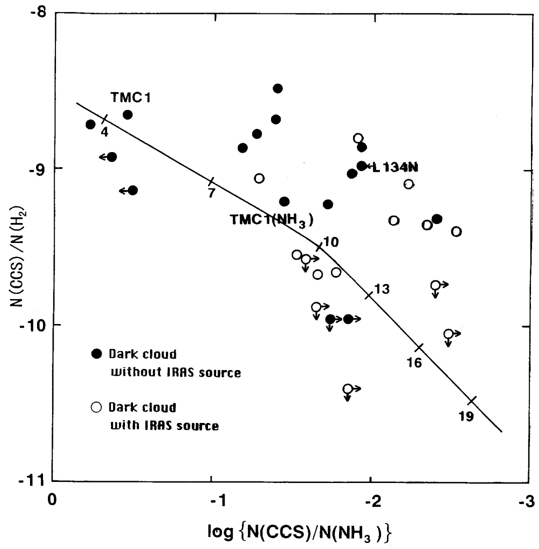

Figure 9. Observed CCS abundance versus the CCS/NH_3 abundance ratio in dark clouds with and without young stars. The solid line indicates the model abundance ratios for T=10 K and $n(H_2)=10^4$ cm^{-3}. The numbers along the line indicate the 'age' of the cloud in 10^5 yr, assuming that the gas is initially atomic-carbon rich (from: Suzuki et al. 1992).

indicates the time since some dynamical event produced an atomic-carbon rich phase.

The model results are also sensitive to the $[C]_g/[O]_g$ elemental abundance ratio in the gas. If this value is increased from the canonical ratio of 0.4 to higher values, improvement with observations for the complex molecules is obtained (Bergin et al. 1997, Terzieva & Herbst 1998). Pratap et al. (1997) show that the observed chemical gradient in TMC-1 can be reproduced by changes in $[C]_g/[O]_g$ along the ridge caused by a density gradient.

This point is further illustrated by high spatial resolution observations of the L1498 pre-stellar core by Kuiper et al. (1996), which show a chemically differentiated structure with NH_3 peaking in the inner region and C_2S in the atomic-carbon rich (clumpy) outer part. Further chemical studies of such cores, especially those which have a more centrally concentrated density structure and appear to be on the verge of collapse (e.g., Ward-Thompson et al. 1994, Motte et al. 1998), are warranted.

The ice mantles in quiescent dark clouds can be probed through the observation of field stars behind the clouds (e.g., Chiar et al. 1995, Whittet et al. 1998). H_2O, CO and CO_2 ices have been detected, which indicate that up to 40% of the heavy elements may be frozen out at densities of a few $\times 10^4$ cm^{-3} (Schutte 1999). Evidence for significant CO depletion deep inside dark clouds ($A_V > 20$ mag) also comes from comparison of $C^{18}O$ observations with extinction maps derived from infrared star counts (Lada et al. 1994, Kramer et al. 1999).

5.3. IONIZATION FRACTION

The ionization fraction $x(e)=n(e)/n(H_2)$ is an important parameter in the dynamical evolution of star-forming regions (see chapters by McKee, Shu, and Mouschovias). In model calculations, x(e) drops from its high value of $\sim 10^{-4}$ at the edge of the core to $\sim 10^{-8}$ in the center, and scales roughly with $(\zeta/n_H)^{1/2}$ (Millar 1990, Bergin & Langer 1997). At the edge, C^+ is the main supplier of electrons, whereas deep inside metal ions such as Mg^+ and Fe^+, as well as molecular ions such as H_3^+, HCO^+ and H_3O^+ dominate.

Recent observations of DCO^+/HCO^+ in a sample of dark cores give ionization fractions of a few $\times 10^{-7}$, for an adopted cosmic ray ionization rate of 5×10^{-17} s^{-1} (Plume et al. 1998, Williams et al. 1998). Surprisingly, no systematic trends between pre-stellar cores and cores with stars have been found, but this may be due to the large scale of the observations ($\sim$10,000 AU). A somewhat lower ionization fraction of 10^{-8}–10^{-7} is found for more massive cores (Bergin et al. 1999, de Boisanger et al. 1996).

6. Chemistry in cold envelopes around YSOs

6.1. MODELS

In the initial stages of collapse, the density increases strongly whereas the temperature stays low, $T \approx 10$ K. The principal prediction of the models is enhanced freeze-out of molecules onto the cold grains under these conditions. The only exceptions are H_2, He, H_3^+ and perhaps N_2. Models appropriate for the cold outer envelopes have been made by Rawlings et al. (1992), Willacy et al. (1994), Bergin & Langer (1997) and Shalabiea & Greenberg (1995), using parametrized fits to the density profiles in simple collapse models such as that of Shu (1977) or Basu & Mouschovias (1994). They differ strongly in the adopted mechanisms that return molecules to the gas, ranging from none in Rawlings et al.'s to efficient desorption in Shalabiea & Greenberg's. The results are also sensitive to the adopted binding energies on the icy mantles, especially whether the outer layer is H_2O-rich or CO-rich. The ions HCO^+ and N_2H^+ are predicted to be good tracers of cold envelopes, because their abundances remain high owing to the increase in the H_3^+ abundance when its main removal partners (CO, O, ...) are depleted. The use of HCO^+ to trace the envelope structure has been demonstrated by Hogerheijde et al. (1997, 1998).

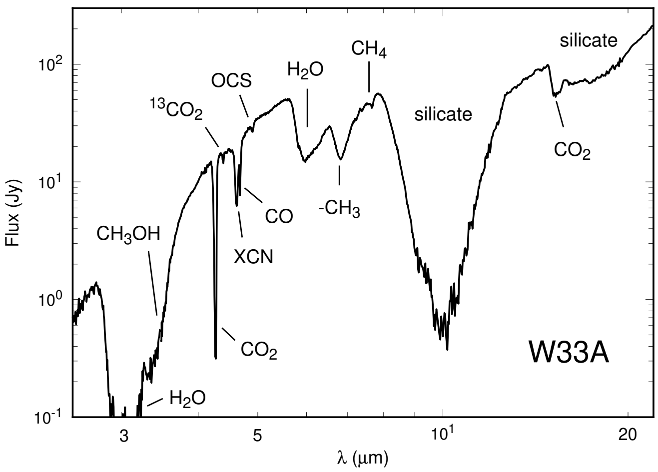

Figure 10. ISO–SWS spectrum of the deeply embedded massive YSO W 33A. Various absorption features due to silicate grain cores and icy mantles are indicated (from: Gibb et al. 1999).

6.2. OBSERVATIONS

Observationally, depletion in collapsing cores is very difficult to prove, because every cloud has a 'skin' in which the abundances are close to normal (Mundy & McMullin 1997). Even if the skin amounts to only a few % of the total column density, its factor of 10–100 higher abundances can effectively mask any depletions deep inside. The dust obscuration in the deeply embedded class 0 stage is still so high that the young stars are too weak at near- and mid-infrared wavelengths for direct observations of ices. Careful modeling of the line and dust emission appears the only way to probe the abundances. One of the best-studied cases is that of NGC 1333 IRAS4, where depletions of more than a factor of 10 have been inferred (Blake et al. 1995). This phase of high depletion appears short-lived, however, since for other class 0 objects like Serpens SMM 1 much less freeze-out has been inferred (see §8.1).

At the more evolved, but still deeply embedded class I stage, infrared absorption line studies of the ice mantles in the cold envelopes become possible, both for low- and high-mass objects (Whittet 1993, Tielens & Whittet 1997, Chiar et al. 1998, Teixeira et al. 1998). Ground-based and ISO studies allow a nearly complete inventory of these ices to be obtained for deeply embedded massive young stars such as NGC 7538 IRS9, W33 A and RAFGL 7009S (Whittet et al. 1996, d'Hendecourt et al. 1996, Ehrenfreund et al. 1997) (see Figure 10). The molecules that have been identified and their typical abundances are summarized in Table 3. Although only abundances down to $\sim 0.5\%$ of H_2O-ice ($\sim 10^{-7}$ with respect to H_2) can be probed, the inferred mantle composition is remarkably simple, consisting of species resulting from the hydrogenation and oxidation of O, C, N and CO. The total column density of gas-phase CO is larger than that of solid CO integrated along the line of sight for all sources studied so far.

7. Chemistry in warm envelopes around newly-formed stars

When a young star begins to heat the inner surrounding envelope by radiation and/or shocks above ~ 100 K, various distinct chemical regions occur, including the hot core region, the region of interaction of the outflow with the surrounding envelope, and the more extended radiatively-heated warm envelope (see Figure 11).

7.1. WARM ENVELOPES

Self-consistent models of the thermal balance, chemistry and radiative transfer in spherical envelopes heated by an internal source have been constructed for low-mass YSO's by Ceccarelli et al. (1996) and for high-mass YSOs by Doty & Neufeld (1997). Calculations of the radial dust temperature distribution include those of Campbell et al. (1995), Kaufman et al. (1998), and van der Tak et al. (1999). For a $\sim 10^5$ $L_\odot$ source, the region where $T_{\rm dust} \approx T_{\rm gas} > 90$ K extends to $\sim 10^{16}$ cm, resulting in evaporation of H_2O and CH_3OH ices and an enhancement of the gas-phase abundances of these species by a factor of 100–1000 (see Figure 11). The chemistry in this inner hot core is discussed in §7.2. The region where $T > 20$ K extends to $\sim 10^{17}$ cm. An increase in the temperature from 10 to 100 K does not have a significant effect on the gas phase chemistry, but does result in evaporation of volatile species like CO.

Observational data on molecules in star-forming regions are scattered throughout the literature, using a variety of (sub-)millimeter telescopes with different beam sizes. Comprehensive single-dish studies of a number of molecules have been performed for only a few sources, including W 3 IRS5 (Helmich & van Dishoeck 1997, see §8.2) and NGC 2264 IRS1 (Schreyer et al. 1997). More detailed physical models are needed to disentangle the contributions of changing temperatures and densities in the envelope from possible radial abundance gradients.

Important complementary information is obtained from high-resolution infrared observations. Mitchell et al. (1990) showed the presence of both cold ($T < 60$ K) and hot ($T = 120$–1000 K) gas along the lines of sight toward massive YSO's from ^{12}CO and ^{13}CO observations. The hot gas contains high abundances of C_2H_2, HCN and CH_4 (Lacy et al. 1989, 1991;

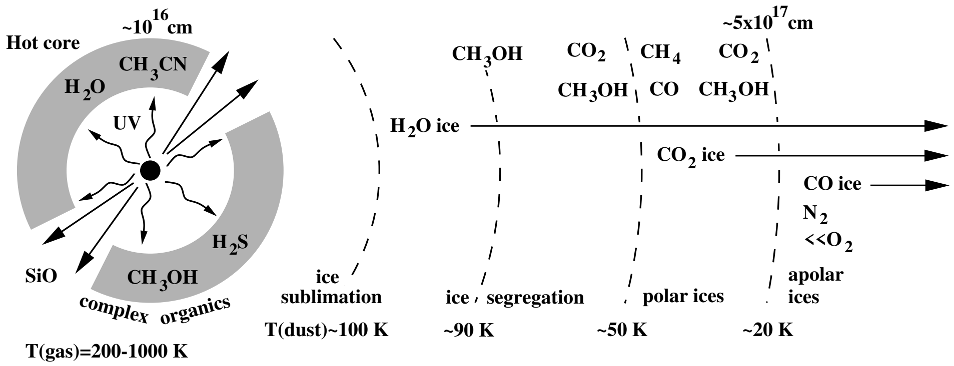

Figure 11. Schematic illustration of the physical and chemical environment of massive YSOs. The variation in the structure of the ice mantles due to heating and thermal desorption is shown (based on Tielens et al. 1991, Williams 1993, van Dishoeck & Blake 1998).

Evans et al. 1991; Carr et al. 1995; Boogert et al. 1998; Lahuis & van Dishoeck 1999), which are enhanced by at least 1–2 orders of magnitude compared with the colder envelope. Gas-phase CO_2 has a surprisingly low abundance (van Dishoeck et al. 1996, Dartois et al. 1998, van Dishoeck 1998b). Clear variations in the gas/solid ratios are seen for various objects, indicating the development of a hot core in the inner envelopes.

7.2. HOT CORE REGIONS

Hot cores are small (<0.1 pc), dense ($n(H_2) > 10^6$ cm^{-3}) and warm ($T \approx$ 200 K or higher) regions located close to massive young stars (see Walmsley & Schilke 1993, Ohishi 1997 for reviews). Observationally, hot cores are characterized by high abundances of fully hydrogenated molecules such as NH_3, H_2S, and H_2O (e.g., Gensheimer et al. 1996), as well as saturated complex organic molecules like CH_3OH, CH_3CN, CH_3OCH_3 and $HCOOCH_3$ (e.g., Hatchell et al. 1998). Examples of hot cores include the Orion hot core and compact ridge (e.g., Blake et al. 1987, Sutton et al. 1995), SgrB2(N) (e.g., Kuan & Snyder 1996), W 3(H_2O) (e.g., Helmich & van Dishoeck 1997) and objects near ultracompact H II regions such as G34.3+0.15 (Macdonald et al. 1996; see chapter by Churchwell). The observed abundances of the species can vary significantly from region to region.

The rich chemistry in hot cores is thought to be driven by the evaporation of icy mantles due to heating near the young star. Charnley et al. (1992) showed that the observed abundances in the Orion hot cores can be reproduced if a mixture of simple ices containing H_2O, CO, CH_3OH, NH_3 and/or HCN is evaporated into the warm gas. These molecules sub-

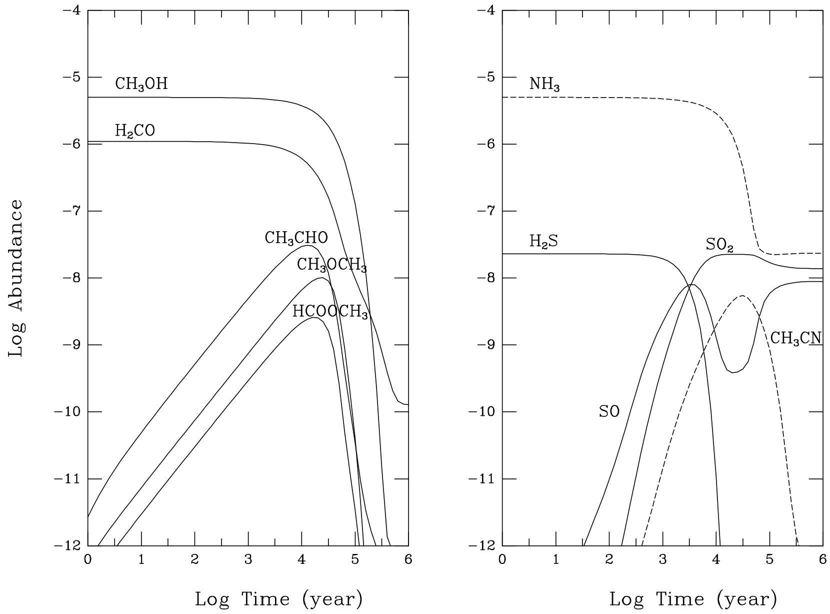

Figure 12. Models of the gas-phase chemical evolution during the 'hot core' phase for T=200 K. At t=0, molecules such as CH_3OH, NH_3 and H_2S are evaporated from the grain mantles into the gas phase, where they drive a rapid chemistry leading to more complex organic molecules such as CH_3OCH_3, $HCOOCH_3$ and CH_3CN. The abundances peak after $10^4 - 10^5$ years (based on Charnley et al. 1992, Charnley 1997).

sequently drive a rapid gas-phase chemistry leading to complex organic molecules (e.g., Charnley et al. 1992, Caselli et al. 1993, Charnley 1997). The abundances of the complex species peak after $\sim 10^4$ yr, thus offering a chemical 'clock' since the time of formation of the hot core (see Figure 12). At later times, the normal ion-molecule chemistry takes over, resulting in destruction of the complex organic molecules after $\sim 10^5$ yr.

Since methanol is one of the most abundant ice mantle consitutents, it plays a crucial role in the hot core chemistry. Specifically, complex oxygen-containing organics can be formed by protonation of CH_3OH by H_3^+, H_3O^+ or HCO^+, followed by transfer of a -CH_3 group to a neutral molecule, e.g., $CH_3OH_2^+ + CH_3OH \rightarrow (CH_3)_2OH^+ + H_2O$. Dissociative recombination of the ion then produces di-methyl ether, CH_3OCH_3. The detailed chemistry of interstellar alcohols leading to large esters and ethers has been discussed by Charnley et al. (1995). Nitrogen-containing organics can be formed through reactions of carbon ions with evaporated NH_3, or through reactions of CN with evaporated C_2H_2. In general, the time scale for formation of nitrogen-rich molecules is somewhat longer than that of oxygen-bearing species.

The H_2S/SO_2 ratio may be a particularly sensitive clock (Charnley 1997, Hatchell et al. 1998). Most of the sulfur is thought to be in the form of H_2S in the ices, although this has not yet been confirmed observationally. Upon evaporation, H_2S is destroyed by reactions with atomic H to atomic S at temperatures of a few hundred K. S can subsequently react with OH and O_2 to form SO and SO_2 on a timescale of $\sim 10^4$ yr. The observed high D/H ratios in hot core molecules (e.g., Millar & Hatchell 1998) largely reflect the high D/H ratios in the ices, which result from the cold dark cloud phase prior to star formation.

7.3. OUTFLOW REGIONS

The earliest stages of star formation are accompanied by powerful outflows, which originate within the young star/accretion disk boundary region. As the high velocity gas flows outward, it strikes the envelope and creates shocks, which alter the chemistry. Recent reviews of the physical and chemical structure of shocks can be found in Draine & McKee (1993), Hollenbach (1997) and Bachiller (1997, this volume).

If the shocks have high velocities (>50 km s^{-1}), the temperature increases to such high values ($> 10^4$ K) that most molecules are collisionally dissociated. In addition, the ultraviolet radiation from such J-type shocks can dissociate molecules both within and ahead of the shock. The molecules reform slowly in a lengthy, warm zone in the wake of the shock (Neufeld & Dalgarno 1989a,b).

For lower shock speeds in clouds with low fractional ionization ($x_e < 10^{-6}$), the shock is of C-type and the temperatures reach peak values of only 2000–3000 K, insufficient to dissociate the molecules. Reactions with energy barriers such as O + H_2 and S + H_2 rapidly drive the available gas-phase oxygen and sulfur into H_2O and H_2S.

In addition to these gas-phase processes, grain cores and mantles are affected by shocks. The high-velocity J-shocks can cause destruction or thermal sputtering of the cores, resulting locally in much enhanced gas-phase abundances of Si, Fe, ... The lower velocity C-shocks can inject a variety of refractory and volatile species into the gas phase through non-thermal sputtering (e.g., Pineau des Forêts & Flower 1997). The released Si can then react with OH and O_2 to form SiO, one of the principal diagnostics of shocks (e.g., Schilke et al. 1997).

Outflows have been studied observationally in a variety of molecules, including H_2 near-infrared emission, CO and SiO. One of the best studied regions chemically is L1157 (Bachiller & Peréz Gutiérrez 1997). Both refractory (SiO, SO, ...) and volatile mantle species (HCN, H_2CO, CH_3OH,

TABLE 4. Physical regions of class 0 YSOs traced by various observations

Region	Observation
Bulk of the (cold) envelope	Interferometer: Continuum on short spacings Single-dish: Lines tracing $T_{\rm kin} < 40$ K (e.g., $C^{18}O$ 2–1; $C^{17}O$ 3–2; $H^{(13)}CO^+$ 3–2, 4–3)
Warm, inner regions of the envelope	Interferometer: Continuum on long spacings Single-dish: Lines tracing ~ 100 K (e.g., ^{13}CO 6–5; H_2CO 3_{22}–2_{21})
Outflow: gradual entrainment (?)	Interferometer: V or U shaped structures (e.g., HCO^+, HCN) Single-dish: line wings (e.g., CO, HCN)
Outflow: direct impact	Single-dish and interferometer: Products of ice mantle evaporation and grain destruction (e.g., SiO, SO)

...) are found to be enhanced in the gas by factors ranging from a few to 10^6. Strong H_2O lines have been observed in outflow regions from the ground (e.g., Cernicharo et al. 1994) and with the ISO satellite, indicating H_2O abundances of a few times 10^{-5} (e.g., Liseau et al. 1996, Ceccarelli et al. 1998, van Dishoeck et al. 1998).

8. Examples

8.1. AN INTERMEDIATE-MASS CLASS 0 YSO IN SERPENS

Recent work by Hogerheijde et al. (1999) of the class 0 YSO Serpens SMM 1 (FIRS 1) illustrates the use of molecular-line and continuum observations with single-dish and aperture-synthesis instruments to constrain the physical and chemical conditions in the envelope of a low- to intermediate-mass protostar. The Serpens molecular cloud ($d \approx 400$ pc) is in the process of forming a loosely bound cluster of more than 50 stars (Eiroa & Casali 1992). SMM 1 is one of the submillimeter-continuum class 0 YSOs identified by Casali et al. (1993) with $L_{\rm bol} = 77\ L_\odot$ and $M_\star = 0.7$–$3.9\ M_\odot$. Table 4 gives an overview of the different physical components traced by the various observations.

The continuum observations are useful to constrain both the mass and the density structure of the envelope. The total mass is derived from the single dish data, whereas the density variation of the envelope is best obtained from the spatially resolved emission in the interferometer. The method is illustrated on the left-hand side of Figure 13. The dependence of the flux on

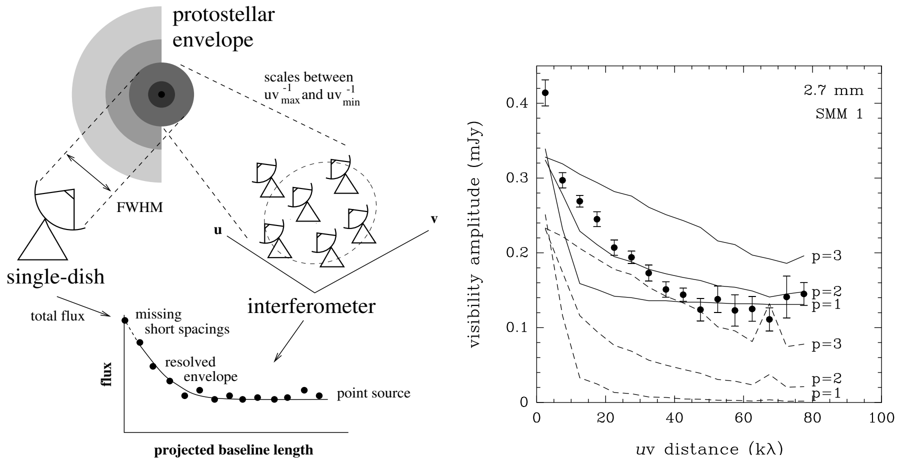

Figure 13. Left: Schematic illustration of single-dish versus interferometer observations. Right: Comparison of model visibility amplitudes at 2.7 mm to observations of SMM 1. The observed vector-averaged amplitudes are indicated by the filled symbols and their 1σ error bars. The dashed lines are models without a central point source, and density power-law slopes of -1.0 (*lower curve in each panel*), -2.0 (*middle curve*), and -3.0 (*upper curve*). Solid lines are models with a point source flux of 0.13 Jy at 2.7 mm and a spectral slope of 2.0.

projected baseline length for SMM 1 (right hand side of Figure 13) indicates a power-law density distribution; different prescriptions like, e.g., a Gaussian distribution, are excluded by the data. A power-law index of -2.0 ± 0.5 gives a good fit to the observations, which agrees well with models for protostellar collapse (e.g., Shu 1977). The fluxes on long baselines suggest the presence of extra, unresolved emission, probably associated with the inner few hundred AU of the envelope where the temperature is likely to exceed the adopted $T_{\rm dust} \propto r^{-0.4}$ distribution. The absolute temperature scale is $\sim$27 K at a characteristic radius of 1000 AU, constrained by the spectral energy distribution over millimeter to far-infrared wavelengths. The total envelope mass is 8.7 $M_\odot$, with an uncertainty of a factor of 2–3 due to the adopted dust emissivity (Ossenkopf & Henning 1994). The fact that the inferred envelope mass is larger than the stellar mass confirms SMM 1's nature as a class 0 YSO.

Using this description for the physical structure of the envelope, the molecular abundances can be determined using models of the line emission. Hogerheijde et al. (1999) adopt a Monte-Carlo technique to solve the radiative transfer and the molecular excitation throughout the envelope. In addition to the physical conditions, the molecular line calculations re-

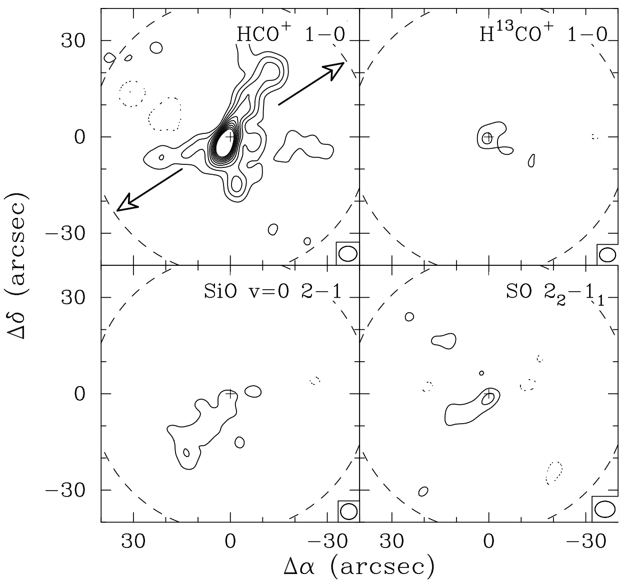

Figure 14. Cleaned, naturally weighted images of molecular line emission observed with OVRO toward SMM 1. Contours are drawn at 3σ intervals, of 1 K km s^{-1} for HCO^+ and SO, 8 K km s^{-1} for $H^{13}CO^+$, and 4 K km s^{-1} for SiO.The synthesized beam size is indicated in each panel. The dashed circle shows the primary beam size. The arrows in the HCO^+ panel indicate the position angle of the radio jet from Rodríguez et al. (1989) (from: Hogerheijde et al. 1999).

quire knowledge of the velocity structure. Systematic velocity fields like infall and outflow can be included, but in the simplest analysis a turbulent line width of $\sim$1.4 km s^{-1} independent of radius is adopted, based on optically thin $C^{17}O$ 3–2 and $H^{13}CO^+$ 3–2 lines. The neglect of systematic velocity fields influences the results for optically thick lines like ^{12}CO and HCO^+. Note that the lines themselves can in principle also constrain the density structure (e.g., Hogerheijde et al. 1997), but are less accurate for low- to intermediate-mass YSOs because of lack of spatial resolution in the single-dish data and of signal-to-noise in the interferometer observations.

The envelope mass can also be constrained from the optically thin CO emission. If the 'standard' dark cloud CO/H_2 abundance of 10^{-4} is adopted, the model overestimates the emission in the $C^{18}O$ 2–1 and $C^{17}O$ 3–2 lines by a factor of 2. Apart from adjusting the CO abundance, a gas kinetic temperature of 0.6 times the dust temperature reconciles this discrepancy; $T_{\rm kin} < T_{\rm dust}$ is expected because of imperfect thermal coupling between the dust and the gas, and line cooling of the gas. Alternatively, CO can freeze out onto dust grains when the temperature drops below its sublimation temperature of $\sim$20 K (see Table 3), lowering the emission. A CO depletion of a factor of 6 in the cold outer layers of the envelope provides a good fit to the $C^{17}O$ 3–2 and $C^{18}O$ 2–1 lines. These lines are particularly good tracers of depletion below 20 K, since the 2–1 lines, tracing $T_{\rm kin} \sim 16$ K gas, are stronger affected than the 3–2 lines, tracing $T_{\rm kin} \sim 30$ K gas. The inferred depletion of a factor of ∼6 for SMM 1 is smaller than found toward other class 0 envelopes (e.g., 10–20 for NGC 1333 IRAS 4, Blake et al. 1995), suggesting that the evolutionary phase characterized by large depletion factors may be short-lived, or that local environment (e.g., heating of the envelope from the outside) influences the depletion.

Most of the observed submillimeter transitions of other molecules trace material in excess of ∼ 30 K, and the derived abundances do not depend critically on the exact value of $T_{\rm kin}$ or possible depletion below 20 K. Table 5 lists the inferred abundances for the parameters of the envelope derived from the dust emission. Compared to other well-studied class 0 YSOs such as IRAS 16293−2422 (van Dishoeck et al. 1995), the abundances of HCO^+, HCN, and H_2CO are very similar, while C_3H_2, CN, and HC_3N are enhanced by an order of magnitude in SMM 1. The values for SiO and SO are lower by a factor of 10, most likely because the $14''$–$19''$ single-dish beam of the SMM 1 observations does not include the tip of the outflow where these species peak (see Figure 14).

Many but not all lines are well fit by this model. High-excitation lines like ^{13}CO 6–5 and H_2CO 3_{22}–2_{21} indicate the presence of an additional amount of warm, ∼ 100 K, material. The estimated column density of this gas amounts to less than 1% of the envelope mass, but dominates in emission of these highly excited lines. It is likely that this material corresponds to the inner few hundred AU of the envelope, where the temperature may exceed the adopted distribution. Some of the emission in the other lines may originate in this component as well. Table 5 includes the abundances derived under the assumption that all emission originates in this warm gas. These values are larger by typically an order of magnitude, illustrating that care needs to be taken to separate these two contributions.

Figure 14 shows the OVRO images of the low-excitation lines of various molecules. The emission in the line wings of optically thick lines of CO, HCO^+ and HCN is clearly associated with the bipolar outflow, as is that of SiO 2–1. HCO^+ outlines the outflow cavity, possibly tracing the slow entrainment of material into the flow. SiO coincides with the axis of the outflow, likely revealing destruction of dust particles by the direct impact of the outflow on ambient material. To derive abundances from these interferometer observations, the modeling has to include spatial filtering. For example, only 0.25 $M_\odot$ is traced by the optically thin $C^{18}O$ 1–0 interferometer observations, but if the resolving-out of extended emission is taken into account, this value is consistent with the total envelope mass

TABLE 5. Derived molecular abundances in the envelope of Serpens SMM 1[a]

Species	Envelope	Warm gas[b]	IRAS 16293−2442[c]
^{12}CO	≡ 1(−4)	≡ 1(−4)	...
HCO^+	1(−9)	2(−8)	2(−9)
HCN	2(−9)	5(−8)	2(−9)
H_2CO	8(−10)	9(−9)	7(−10)
C_3H_2	2(−10)	3(−9)	4(−11)
CN	5(−9)	3(−8)	1(−10)
HC_3N	2(−10)	9(−10)	3(−11)
SiO	1(−11)	1(−10)	1(−10)
SO	2(−10)	2(−9)	4(−9)

[a] From Hogerheijde et al. (1999).
[b] Abundances derived under the assumption that *all* emission originates in warm 100 K gas.
[c] From van Dishoeck et al. (1995).

of 8.7 $M_\odot$. Firmer conclusions about abundance variations on small scales requires more realistic, >1D models of the physical structure, including a correct treatment of the velocity field.

8.2. THE W 3 MASSIVE STAR-FORMING REGION

The W 3 massive star-forming region at $\sim$ 2.3 kpc provides an excellent opportunity to study the chemistry of massive YSOs ($L \approx 10^5 L_\odot$) at different evolutionary stages originating from the same parent cloud. Helmich et al. (1994) and Helmich & van Dishoeck (1997) performed an unbiased single-dish submillimeter spectral survey of three YSOs at 15″ (0.15 pc) resolution: IRS5, IRS4 and W 3(H_2O). Although such observations lack the spatial resolution of the data on nearby low-mass objects discussed above, they provide a useful global picture of the chemistry. In addition, the envelope mass associated with these objects is significantly larger than for low-mass YSOs, so that even minor species can be detected.

Figure 15 summarizes the spectra toward the three objects in the 345 GHz atmospheric window. Clear physical and chemical differences are found between the three sources, in spite of their similar luminosities. The beam-averaged densities are at least 10^6 cm^{-3} and the temperatures range from $\sim$ 55 K for IRS4 to at least 220 K for W 3(H_2O). Toward W 3(IRS5), silicon- and sulfur-bearing molecules such as SiO and SO_2 are prominent. This source has a powerful, massive outflow and is presumably the youngest of

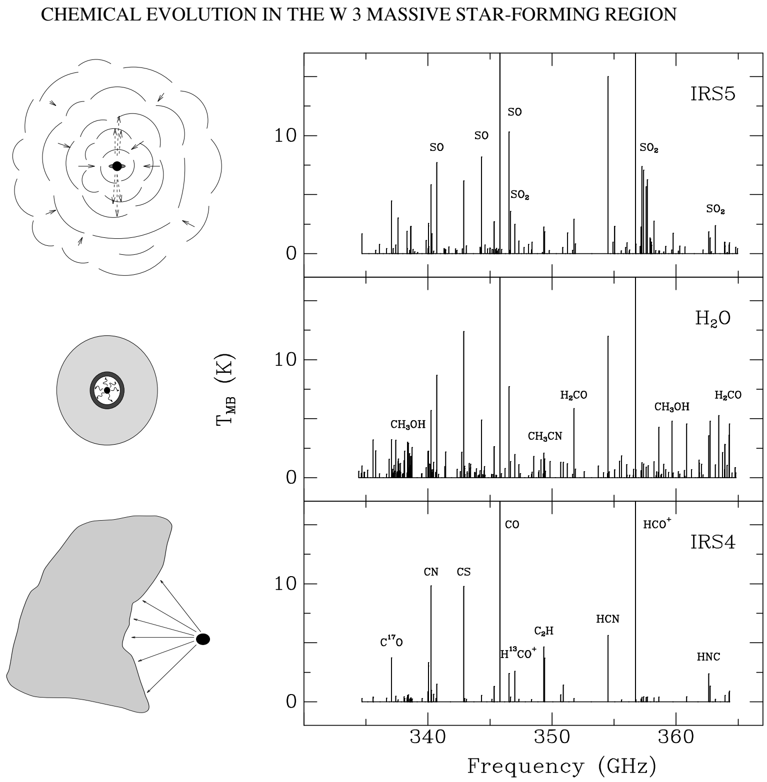

Figure 15. Summary of the JCMT 335–365 GHz line survey of three massive star–forming regions in the W 3 molecular cloud. The spectra were constructed from the observed line intensities obtained in double–side-band mode. Strong lines in common in the three spectra are labelled in the W 3 IRS4 spectrum only. Large physical and chemical differences are found between the three regions, which are attributed to different evolutionary stages (Based on Helmich & van Dishoeck 1997).

the three sources, showing also strong ice absorption features in its infrared spectra. Toward W 3(H_2O), discovered by Turner & Welch (1984), organic molecules like CH_3OH, CH_3OCH_3, and CH_3OCHO are at least one order of magnitude more abundant, indicating that it is well into the hot core phase. Finally, only simple molecules and radicals are found toward IRS4. One possible interpretation is that this object is more evolved and has already broken free from the parent cloud, setting up an H II region and PDR on the back side of the cloud.

More detailed physical models, which constrained by multi-line observations of high-dipole molecules like CS, H_2CO, HCN and their isotopes, are needed to infer reliable abundances. Recent analyses of the massive YSO GL 2591 suggest a power-law density distribution with an index of -1.0 to -1.5, somewhat shallower than found for low-mass YSOs such as SMM 1 (Carr et al. 1995, van der Tak et al. 1999).

9. Chemistry in circumstellar disks

Most of this chapter has focused on the chemistry in the envelopes of deeply-embedded YSOs. Young stars with ages $1-5$ Myr have dispersed their envelopes but are still surrounded by circumstellar disks with masses of $\sim 10^{-3}-10^{-1}$ $M_\odot$ and sizes of $\sim$100 AU, comparable to those inferred for our primitive solar nebula (see Beckwith & Sargent 1996 for a review). Imaging of the gas in disks around T Tauri and Herbig Ae stars has so far been limited to CO and its isotopes, for reasons of sensitivity. Observations of other molecules are only just beginning. Single-dish surveys of various molecules have been carried out for a few objects, in particular DM Tau and GG Tau (Dutrey et al. 1997), TY Hya (Kastner et al. 1997) and LkCa 15, MWC 480 and HD 163296 (Thi et al., in preparation). Millimeter interferometers are now also capable of imaging the more abundant molecules in disks, showing interesting morphological differences (Qi et al., in preparation).

The detection of species like HCO^+, CN and HNC indicates that both ion-molecule, photon-dominated and gas-grain chemistry play a role. The amount of depletion is high because of the high densities (typically 10^6-10^9 cm^{-3} in the outer disk) and appears to be species-dependent, with the most volatile molecules remaining in the gas furthest from the central star. Chemical models which couple the gas-dust chemistry with the dynamical evolution as the material is transported inwards have been developed recently by Aikawa et al. (1997, 1998) and Willacy et al. (1998). At small disk radii, irradiation from the central star and stellar X-rays may also affect the chemistry. These studies are important first steps to determine the connection between interstellar and solar nebula processes in the formation of icy planetesimals such as comets and Kuiper-Belt objects.

10. Concluding remarks

Significant progress has been made in the last decade on models and observations of the chemistry in star-forming regions. New (sub-)millimeter data at higher angular resolution and frequencies allow the dense and warm components of the YSO envelopes to be probed directly. Ground- and spaced-based infrared observations provide the first complete inventory of solid-state species along the line of sight and put constraints on gas/solid ratios of abundant species. The large variations in observed abundances illustrate that the chemistry clearly responds to the enormous changes in temperature and density during star-formation. Molecules freeze out onto grains in the cold pre-stellar cores and outer envelopes surrounding YSOs, where grain-surface chemistry produces new species. They are returned to the gas by heating due to radiation from the young stars and by shocks due to outflows impacting on the envelope. A rich chemistry can ensue in the hot gas, leading to abundant complex organic molecules and driving much of the available oxygen into water. Thus, these molecules provide important chemical and temporal diagnostics of the YSO environment.

The derivation of abundances from spectral line data is far from simple, however, and invariably includes assumptions about the underlying source structure. This physical structure can be constrained by analyzing spatially resolved continuum data, as illustrated for the case of Serpens SMM 1, and by using line ratios of appropriate molecules to infer temperatures and densities. Different approaches, ranging from the "homogeneous" to the "detailed" method, offer optimal strategies for different cases. Interferometric data require special care, because the instrument is a spatial filter which acts differently on lines tracing different physical conditions.

The development of comprehensive gas–grain models has made it possible to put the observational results into a coherent framework of the evolution of gas and solid species throughout the formation of protostars to their incorporation into circumstellar disks and eventually comets and planetesimals. Such models are rapidly progressing beyond the (pseudo) time-dependent method, and attempts are being made to couple the chemistry with (multi-)dimensional hydrodynamics. Accurate information on the basic molecular processes entering such models remains a prerequisite.

Future instrumentation, such as the next generation submillimeter arrays and air- or space-borne infrared telescopes such as SOFIA, SIRTF, FIRST and NGST, will allow these studies to be extended to much higher sensitivity and/or smaller scales of only a few AU. Together they should provide a much clearer view on the connection between matter found in interstellar clouds and in new planetary systems, and on the origin of organic matter found in primitive objects in our own solar system.

Acknowledgements

The authors are grateful to many colleagues for discussions and preprints of their work. They are indebted to the Leids Kerkhoven-Bosscha Fonds and the organizers for financial support. Research on Astrochemistry in Leiden is supported by the Netherlands Organization for Scientific Research (NWO). MRH is supported by the Miller Institute for Basic Research in Science.

References

Aikawa, Y., Umebayashi, T., Nakano, T., Miyama, S.M. (1997), *ApJ*, **486**, p. L51
Aikawa, Y., Umebayashi, T., Nakano, T., Miyama, S.M. (1998), *Faraday Disc.*, **109**, p. 281
Bachiller, R. (1997), in *Molecules in Astrophysics: Probes and Processes*, IAU Symposium 178, ed. E.F. van Dishoeck. Kluwer Academic Publishers, Dordrecht, p. 103
Bachiller, R. and Peréz Gutiérrez, M. (1997), *ApJ*, **487**, p. L93
Basu, S. and Mouschovias, T.C. (1994), *ApJ*, **432**, p. 720
Beckwith, S.V.W. and Sargent, A.I. (1996), *Nature*, **383**, p. 139
Benson, P.J., Caselli, P. and Myers, P.C. (1998), *ApJ*, **506**, p. 743
Bergin, E.A. and Langer, W.D. (1997), *ApJ*, **486**, p. 316
Bergin, E.A., Goldsmith, P.F., Snell, R.L. and Langer, W.D. (1997), *ApJ*, **482**, p. 285
Bergin, E.A., Plume, R., Williams, J.P. and Myers, P.C. (1999), *ApJ*, in press
Bernes, C. (1979), *A&A*, **73**, p. 67
Bernstein, M.P., Sandford, S.A., Allamandola, L.J., Chang, S. and Scharberg, M.A. (1995), *ApJ*, **454**, p. 327
Blake, D., Allamandola, L., Sandford, S., Hudgins, D., Freund, F. (1991), *Science*, **254**, pp. 548
Blake, G.A. (1997), in *Molecules in Astrophysics: Probes and Processes*, IAU Symposium 178, ed. E.F. van Dishoeck, Kluwer Academic Publishers, Dordrecht, p. 31
Blake, G.A., Sandell, G., van Dishoeck, E.F., Groesbeck, T.D., Mundy, L.G. and Aspin, C. (1995), *ApJ*, **441**, p. 689
Blake, G.A., Sutton, E.C., Masson, C.R. and Phillips, T.G. (1987), *ApJ*, **315**, p. 621
Boogert, A.C.A., Helmich, F.P., van Dishoeck, E.F., Schutte, W.A., Tielens, A.G.G.M. and Whittet, D.C.B. (1998), *A&A*, **336**, p. 352
Boogert, A.C.A., Ehrenfreund, P., Gerakines, P., et al. (1999), *A&A*, in press
Campbell, M.F., Butner, H.M., Harvey, P.M., Evans, N.J., Campbell, M.B. and Sabbey C.N. (1995), *ApJ*, **454**, p. 831
Carr, J.S., Evans, N.J., Lacy, J.L. and Zhou, S. (1995), *ApJ*, **450**, p. 667
Casali, M.M., Eiroa, C. and Duncan, W.D. (1993), *A&A*, **275**, p. 195
Caselli, P., Hasegawa, T.I. and Herbst, E. (1993), *ApJ*, **408**, p. 548
Caselli, P., Hasegawa T.I. and Herbst, E. (1998), *ApJ*, **495**, p. 309
Ceccarelli, C., Hollenbach, D.J. and Tielens, A.G.G.M. (1996), *ApJ*, **471**, p. 400
Ceccarelli, C., Castets, A., Loinard, L., Caux, E. and Tielens, A.G.G.M. (1998), *A&A*, **338**, p. L43
Cernicharo, J., González-Alfonso, E., Alcolea, J., Bachiller, R. and John, D. (1994), *ApJ*, **432**, p. L59
Charnley, S.B. (1997), *ApJ*, **481**, p. 396
Charnley, S.B, Kress, M.E., Tielens, A.G.G.M. and Millar, T.J. (1995), *ApJ*, **448**, p. 232
Charnley, S.B., Tielens, A.G.G.M. and Millar, T.J. (1992), *ApJ*, **399**, p. L71
Chiar, J.E., Adamson, A.J., Kerr, T.H. and Whittet, D.C.B. (1995), *ApJ*, **455**, p. 234
Chiar, J.E., Gerakines, P.A., Whittet, D.C.B., Pendleton, Y.J., Tielens, A.G.G.M., Adamson, A.J. and Boogert, A.C.A. (1998), *ApJ*, **498**, p. 716
Dalgarno, A. (1987), in *Physical Processes in Interstellar Clouds*, eds. G. Morfill and M.S. Scholer, D. Reidel, Dordrecht, p. 219
Dalgarno, A. (1994), *Adv. At. Mol. & Opt. Phys.*, **32**, p. 57
Dartois, E., d'Hendecourt, L., Boulanger, F., Jourdain de Muizon, M., Breitfellner, M., Puget, J.-L., and Habing, H.J. (1998), *A&A*, **331**, p. 651
de Boisanger, C., Helmich, F.P. and van Dishoeck, E.F. (1996), *A&A*, **310**, p. 315
d'Hendecourt, L., Jourdain de Muizon, M., Dartois, E., Breitfellner, M., Ehrenfreund, P., Benit, J., Boulanger, F., Puget, J.L. and Habing H.J. (1996), *A&A*, **315**, p. L365
Doty, S.D. and Neufeld, D.A. (1997), *ApJ*, **489**, p. 122
Draine, B.T. (1978), *ApJS*, **36**, p. 595
Draine, B.T. and McKee, C.F. (1993), *ARA&A*, **31**, p. 373

Dutrey, A., Guilloteau, S. and Guélin, M. (1997), *A&A*, **317**, p. L55
Eiroa, C. and Casali, M.M. (1992), *A&A*, **262**, p. 468
Ehrenfreund, P., d'Hendecourt, L., Dartois, E., Jourdain de Muizon, M., Breitfellner, M., Puget, J.L. and Habing, H.J. (1997), *Icarus*, **130**, p. 1
Ehrenfreund, P., Dartois, E., Demyk, K. and d'Hendecourt, L. (1998), *A&A*, **339**, p. L17
Evans, N.J. (1980), in *Interstellar Molecules*, Proc. IAU 87, ed. B.H. Andrew, D. Reidel, Dordrecht, p. 1
Evans, N.J., Lacy, J.H. and Carr, J.S. (1991), *ApJ*, **383**, p. 674
Flower, D. (1990). Molecular Collisions in the Interstellar Medium, Cambridge University Press
Frerking, M.A., Langer, W.D. and Wilson, R.W. (1982), *ApJ*, **262**, p. 590
Geballe, T.R. and Oka, T. (1996), *Nature*, **384**, p. 334
Gensheimer, P.D., Mauersberger, R. and Wilson, T.L. (1996), *A&A*, **314**, p. 281
Genzel, R. (1992), in *The Galactic Interstellar Medium*, eds. D. Pfenniger and P. Bartholdi, Saas Fee Advanced Course 21, Springer, Berlin, p. 275
Gerakines, P.A., Schutte, W.A. and Ehrenfreund, P. (1996), *A&A*, **312**, p. 289
Gerakines, P.A., Whittet, D.C.B., Ehrenfreund, P. et al. (1999), *ApJ*, in press
Gibb, E., Whittet, D.C.B., et al. (1999), in preparation
Gredel, R., van Dishoeck, E.F. and Black, J.H. (1993), *A&A*, **269**, p. 477
Gredel, R., Lepp, S., Dalgarno, A. and Herbst, E. (1989), *ApJ*, **347**, p. 289
Green, S. (1975), in Atomic and molecular physics and the interstellar matter, ed. R. Balian et al., Elsevier North Holland, Amsterdam, p. 83
Habing, H.J. (1988), in *Millimetre and Submillimetre Astronomy*, ed. R.D. Wolstencroft and W.B. Burton , Kluwer Academic Publishers, Dordrecht, p. 207
Hartquist T.W., Caselli, P., Rawlings, J.M.C., Ruffle, D.P., Williams, D.A. (1998), in *The Molecular Astrophysics of Stars and Galaxies*, ed. T.W. Hartquist and D.A. Williams, Oxford, Oxford University, p. 101
Hasegawa, T.I. and Herbst, E. (1993), *MNRAS*, **261**, p. 83
Hatchell, J., Thompson, M.A., Millar, T.J. and Macdonald, G.H. (1998), *A&AS*, **133**, 29
Helmich, F.P. and van Dishoeck, E.F. (1997), *A&AS*, **124**, p. 205
Helmich, F.P., Jansen, D.J., de Graauw, Th., Groesbeck, T.D. and van Dishoeck, E.F. (1994), *A&A*, **283**, p. 626
Herbst, E. (1993), in *Dust and Chemistry in Astronomy*, eds. T.J. Millar and D.A. Williams, IOP, Bristol, p. 183
Herbst, E. (1995), *Ann. Rev. Phys. Chem.*, **46**, p. 27
Herbst, E. and Leung, C.M. (1986), ApJ, **310**, 378.
Herbst, E. and Klemperer, W. (1973), *ApJ*, **185**, p. 505
Hogerheijde, M.R., Jansen, D.J. and van Dishoeck, E.F. (1995), *A&A*, **294**, p. 792
Hogerheijde, M.R., van Dishoeck, E.F., Blake, G.A. and van Langevelde, H.J. (1997), *ApJ*, **489**, p. 293
Hogerheijde, M.R., van Dishoeck, E.F., Blake, G.A. and van Langevelde, H.J. (1998), *ApJ*, **502**, p. 315
Hogerheijde, M.R., van Dishoeck, E.F., Salverda, J.M. and Blake, G.A. (1999), *ApJ*, in press
Hollenbach, D.J. (1997), in *Herbig-Haro Objects and the Birth of Low-mass Stars, IAU Symposium 182*, ed. B. Reipurth & C. Bertout, Kluwer Academic Publishers, Dordrecht, p. 181
Hollenbach, D.J. and Salpeter, E.E. (1971), *ApJ*, **163**, p. 155
Hollenbach, D.J. and Tielens, A.G.G.M. (1997), *ARA&A*, **35**, p.179
Hollenbach, D.J. and Tielens, A.G.G.M. (1999), *Rev. Mod. Phys.*, in press
Irvine, W.M. (1998), in *Origins of Life and Evolution of the Biosphere*, **28**, p. 365
Irvine W.M., Schloerb, F.P., Crovisier, J., Fegley, B., and Mumma, M.J. (1999), *Protostars & Planets IV*, eds. V.G. Mannings and S. Russell, University of Arizona, in press

Kaiser, R.I. and Roessler, K. (1997), *ApJ*, **475**, p. 487
Kaiser, R.I., Stranges, D., Lee, Y.T. and Suits, A.G. (1997), *ApJ*, **477**, p. 982
Kastner, J.H., Zuckerman, B., Weintraub, D.A. and Forveille, T. (1997), *Science*, **277**, p. 67
Kaufman, M.J., Hollenbach, D.J. and Tielens, A.G.G.M. (1998), *ApJ*, **497**, p. 276
Kramer, C., Alves, J., Lada, C.J., Lada, E.A., Sievers, A., Ungerechts, H. and Walmsley, C.M. (1999), *A&A*, **329**, p. L33
Kuan, Y.J. and Snyder, L.E. (1996), *ApJ*, **470**, p. 981
Kuiper, T.B.H., Langer, W.D. and Velusamy, T. (1996), *ApJ*, **468**, p. 761
Lacy, J.H., Carr, J.S., Evans, N.J., Baas, F., Achtermann, J.M. and Arens, J.F. (1991), *ApJ*, **376**, p. 556
Lacy, J.H., Evans, N.J., Achtermann, J.M., Bruce, D.E., Arens, J.F. and Carr, J.S. (1989), *ApJ*, **342**, p. L43
Lacy, J.H., Knacke, R., Geballe, T.R. and Tokunaga, A.T. (1994), *ApJ*, **428**, p. L69
Lacy, J.H., Faraji, H., Sandford, S.A. and Allamandola, L.J. (1998), *ApJ*, **501**, p. L105
Lada, C.J., Lada, E.A., Clemens, D. and Bally, J. (1994). *ApJ*, **429**, p. 694
Lahuis, F. and van Dishoeck, E.F. (1999), *A&A*, to be submitted
Langer, W.D., Velusamy, T., Kuiper, T.B.H., Peng, R., McCarthy, M.C., Travers, M.J., Kovacs, A., Gottlieb, C.A. and Thaddeus, P. (1997), *ApJ*, **480**, p. L63
Langer, W.D., van Dishoeck, E.F., Blake, G.A. et al. (1999), *Protostars & Planets IV*, eds. V.G. Mannings and S. Russell, University of Arizona, in press
Larsson, M. (1997), *Ann. Rev. Phys. Chem.*, **48**, 151
le Bourlot, J., Pineau des Forêts, G., Roueff, E. and Flower, D.R. (1995), *A&A*, **302**, p. 870
Lee, H.-H., Bettens, R.P.A. and Herbst, E. (1996a), *A&AS*, **119**, p. 111
Lee, H.-H., Herbst, E., Pineau des Forêts, G., Roueff, E. and le Bourlot, J. (1996b), *A&A*, **311**, p. 690
Lee, H.-H., Roueff, E., Pineau des Forêts, G., Shalabiea, O., Terzieva, R. and Herbst, E. (1998), *A&A*, **334**, p. 1047
Liseau, R., Ceccarelli, C., Larsson, B. et al. (1996), *A&A*, **315**, p. L181
Lucas, R. and Liszt, H. (1997), in *Molecules in Astrophysics: Probes and Processes*, IAU Symposium 178, ed. E.F. van Dishoeck, Kluwer Academic Publishers, Dordrecht, p. 421
Macdonald, G.H., Gibb, A.G., Habing, R.J. and Millar, T.J. (1996), *A&AS*, **119**, p. 333
Maloney, P.R., Hollenbach, D.J. and Tielens, A.G.G.M. (1996), *ApJ*, **466**, p. 561
Marechal, P., Pagani, L., Langer, W.D. and Castets, A. (1997), *A&A*, **318**, p. 252
McCall, B.J., Hinkle, K.H., Geballe, T.R. and Oka, T. (1998), *J. Chem Soc. Far. Disc.*, **109**, p. 267
Melnick, G., Stauffer, J.R., Ashby, M. et al. (1998), BAAS, 193, 72.01
Meyer, D.M. (1997), in *Molecules in Astrophysics: Probes and Processes*, IAU Symposium 178, ed. E.F. van Dishoeck, Kluwer Academic Publishers, Dordrecht, p. 407
Millar, T.J. (1990), in *Molecular Astrophysics —A volume honoring Alexander Dalgarno*, ed. T.W. Hartquist, Cambridge University Press, p. 115
Millar, T.J., Bennett, A. and Herbst, E. (1989), *ApJ*, **340**, p. 906
Millar, T.J., Farquhar, P.R.A. and Willacy, K. (1997a), *A&AS*, **121**, p. 139
Millar, T.J., Macdonald, G.H. and Gibb, A.G. (1997b), *A&A*, **325**, p. 1163
Millar, T.J. and Hatchell, J. (1998), *J. Chem Soc. Far. Disc.*, **109**, p. 15
Mitchell, G.F., Maillard, J.-P., Allen, M., Beer, R. and Belcourt, K. (1990), *ApJ*, **363**, p. 554
Moore, M.H., Donn, B., Khanna, R. and A'Hearn, M.F. (1983), *Icarus*, **54**, p. 388
Motte, F., André, P. and Neri, R. (1998), *A&A*, **336**, p. 150
Mundy, L. and McMullin, J.P. (1997), in *Molecules in Astrophysics: Probes and Processes*, IAU Symposium 178, ed. E.F. van Dishoeck, Kluwer Academic Publishers, Dordrecht, p. 183
Myers, P.C. and Benson, P.J. (1983), *ApJ*, **266**, p. 309

Neufeld, D.A. and Dalgarno, A. (1989a), *ApJ*, **340**, p. 869
Neufeld, D.A. and Dalgarno, A. (1989b), *ApJ*, **344**, p. 251
Ohishi, M. (1997), in *Molecules in Astrophysics: Probes and Processes*, IAU Symposium 178, ed. E.F. van Dishoeck, Kluwer Academic Publishers, Dordrecht, p. 61
Olano, C.A., Walmsley, C.M. and Wilson, T.L. (1988), *A&A*, **196**, p. 194
Olofsson, G., Pagani, L., Tauber, J., et al. (1998), *A&A*, **339**, p. 81
Ossenkopf, V. and Henning, T. (1994), *A&A*, **291**, p. 943
Osterbrock (1989), *Astrophysics of Gaseous Nebulae and Active Galactic Nuclei*, University Science Books, Mill Valley
Pineau des Forêts, G. and Flower, D.R. (1997), in *Molecules in Astrophysics: Probes and Processes*, IAU Symposium 178, ed. E.F. van Dishoeck, Kluwer Academic Publishers, Dordrecht, p. 113
Plume, R., Bergin, E.A., Williams, J.P. and Myers, P.C. (1998), *J. Chem Soc. Far. Disc.*, **109**, p. 47
Prasad, S.S. and Huntress, W.T. (1980), *ApJS*, **43**, p. 1
Pratap, P., Dickens, J.E., Snell, R.L. et al. (1997), *ApJ*, **486**, p. 862
Rawlings, J.M.C., Hartquist, T.W., Menten, K.M. and Williams, D.A. (1992), *MNRAS*, **255**, p. 471
Roberge, W.G., Jones, D., Lepp, S. and Dalgarno, A. (1991), *ApJS*, **77**, p. 287
Rodríguez, L.F., Curiel, S., Moran, J., Mirabel, I.F., Roth, M. and Garay, G. (1989), *ApJ*, **346**, p. L85
Sandford, S.A. and Allamandola, L.J. (1990), *Icarus*, **87**, p. 188
Sandford, S.A. and Allamandola, L.J. (1993), *ApJ*, **417**, p. 815
Schilke, P., Walmsley, C.M., Pineau des Forêts, G. and Flower, D.R. (1997), *A&A*, **321**, p. 293
Schreyer, K., Helmich, F.P., van Dishoeck, E.F. and Henning, T. (1997), *A&A*, **326**, p. 347
Schutte, W.A. (1996), in *The Cosmic Dust Connection*, ed. J.M. Greenberg, Kluwer Academic Publishers, Dordrecht, p. 1
Schutte, W.A. (1999), in *Laboratory astrophysics and space missions*, eds. P. Ehrenfreund et al., Kluwer Academic Publishers, Dordrecht, p. 69
Schutte, W.A., Tielens, A.G.G.M. and Allamandola, L.J. (1993), *ApJ*, **415**, p. 397
Shalabiea, O. and Greenberg, J.M. (1995), *A&A*, **296**, p. 779
Shalabiea, O.M., Caselli, P. and Herbst, E. (1998), *ApJ*, **502**, p. 652
Shu, F.H. (1977), *ApJ*, **214**, p. 488
Shu, F.H., Adams, F.C., and Lizano, S. (1987), *ARA&A*, **25**, p. 23
Smith, I.W.M. (1997), in *Molecules in Astrophysics: Probes and Processes*, IAU Symposium 178, ed. E.F. van Dishoeck, Kluwer Academic Publishers, Dordrecht, p. 253
Sobolev, V.V. (1960), *Moving Envelopes of Stars*, Harvard University Press, Cambridge
Sternberg, A., Yan, M. and Dalgarno, A. (1997), in *Molecules in Astrophysics: Probes and Processes*, IAU Symposium 178, ed. E.F. van Dishoeck, Kluwer Academic Publishers, Dordrecht, p. 141
Sutton, E.C., Peng, R., Danchi, W.C., Jaminet, P.A., Sandell, G., and Russell, A.P.G. (1995), *ApJS*, **97**, p. 455
Suzuki, H., Yamamoto, S., Ohishi, M. et al., (1992), *ApJ*, **392**, p. 551
Teixeira, T.C., Emerson, J.P. and Palumbo, M.E. (1998), *A&A*, **330**, p. 711
Terzieva, R. and Herbst, E. (1998), *ApJ*, **501**, p. 207
Tielens, A.G.G.M. (1983), *A&A*, **119**, p. 177
Tielens, A.G.G.M. and Allamandola, L.J. (1987), in *Interstellar Processes*, eds. D. Hollenbach and H.A. Thronson, D. Reidel, Dordrecht, p. 379
Tielens, A.G.G.M. and Charnley, S.B. (1997), *Origin of Life*, **27**, p. 23
Tielens, A.G.G.M. and Hagen, W. (1982), *A&A*, **114**, p. 245
Tielens, A.G.G.M., Tokunaga, A.T., Geballe, T.R. and Baas, F. (1991), *ApJ*, **381**, p. 181
Tielens, A.G.G.M. and Whittet, D.C.B. (1997), in *Molecules in Astrophysics: Probes and Processes*, IAU Symposium 178, ed. E.F. van Dishoeck, Kluwer Academic Publishers,

Dordrecht, p. 45
Turner, B.E. (1996), *ApJ*, **468**, p. 694.
Turner, B.E. (1998), *ApJ*, **495**, p. 804
Turner, B.E., Lee, H.H. and Herbst, E. (1998), *ApJS*, **115**, p. 91
Turner, J.L. and Welch, W.J. (1984), *ApJ*, **287**, p. L81
Vandenbusssche, B., Ehrenfreund, P., Boogert, A.C.A., et al. (1999), *A&A*, submitted
van der Tak, F., van Dishoeck, E.F., Evans, N.J., Bakker, E. and Blake, G.A. (1999), *ApJ*, submitted
van Dishoeck, E.F. (1988), in *Millimetre and Submillimetre Astronomy*, ed. R.D. Wolstencroft and W.B. Burton, Kluwer Academic Publishers, Dordrecht, p. 117
van Dishoeck, E.F. (1998a), in *The Molecular Astrophysics of Stars and Galaxies*, ed. T.W. Hartquist and D.A. Williams, Oxford, Oxford University, p. 53
van Dishoeck, E.F. (1998b), *Faraday Disc.*, **109**, p. 31
van Dishoeck, E.F. and Black, J.H. (1987), in *Physical Processes in Interstellar Clouds*, eds. G. Morfill and M.S. Scholer, D. Reidel, Dordrecht, p. 241
van Dishoeck, E.F. and Black, J.H. (1988), *ApJ*, **334**, p. 771
van Dishoeck, E.F. and Blake, G.A. (1998), *ARA&A*, **36**, p. 317
van Dishoeck, E.F., Blake, G.A., Draine, B.T., Lunine, J.I. (1993), in *Protostars and Planets III*, eds. E.H. Levy and J.I. Lunine, Univ. of Arizona, p. 163
van Dishoeck, E.F., Blake, G.A., Jansen, D.J. and Groesbeck, T.D. (1995), *ApJ*, **447**, p. 760
van Dishoeck, E.F., Helmich, F.P., de Graauw, Th. et al. (1996), *A&A*, **315**, p. L349
van Dishoeck, E.F., Wright, C.M., Cernicharo, J., et al. (1998), *ApJ*, **502**, p. L173
van Dishoeck, E.F., Helmich, F.P., Schutte, W.A., et al. 1998, in *Star Formation with the Infrared Space Observatory*, eds. J. Yun and R. Liseau, ASP vol. 132, p. 54
Vejby-Christensen, L., Andersen, L.H., Heber, O., Kella, D., Pedersen, H.B., Schmidt, H. and Zajfman, D. (1997), *ApJ*, **483**, p. 531
Walmsley, C.M. (1987), in *Physical Processes in Interstellar Clouds*, eds. G. Morfill and M.S. Scholer, D. Reidel, Dordrecht, p. 161
Walmsley, C.M. (1991), in *Fragmentation of molecular clouds and star formation*, IAU Symposium 147, eds. E. Falgarone et al., Kluwer Academic Publishers, Dordrecht, p. 161
Walmsley, C.M. and Schilke, P. (1993), in *Dust and Chemistry in Astronomy*, eds. T.J. Millar and D.A. Williams, IOP Publishing, Bristol, p. 37
Ward-Thompson, D., Scott, P.F., Hills, R.E. and André, P. (1994), *MNRAS*, **268**, p. 276
Whittet, D.C.B. (1993), in *Dust and Chemistry in Astronomy*, eds. T.J. Millar and D.A. Williams, IOP Publishing, Bristol, p. 9.
Whittet, D.C.B., Gerakines, P.A., Tielens, A.G.G.M. et al. (1998), *ApJ*, **498**, p. L159
Whittet, D.C.B., Schutte, W.A., Tielens, A.G.G.M. et al. (1996), *A&A*, **315**, p. L357
Willacy, K.R., Rawlings, J.M.C. and Williams, D.A. (1994), *MNRAS*, **269**, p. 921
Willacy, K.R., Klahr, H.H., Millar, T.J. and Henning, Th. (1998), *A&A*, **338**, p. 995
Williams, D.A. (1993), in *Dust and Chemistry in Astronomy*, eds. T.J. Millar and D.A. Williams, IOP Publishing, Bristol, p. 143
Williams, J.P., Bergin, E.A., Caselli, P., Myers, P.C. and Plume, R. (1998), *ApJ*, **503**, p. 689
Wootten, A. (1987), in *Astrochemistry*, eds. M.S. Vardya and S.P. Tarafdar, Kluwer Academic Publishers, Dordrecht, p. 311